Received: 15 July 2025 | Revised: 9 October 2025 | Accepted: 21 October 2025 | Published online: 6 November 2025

RESEARCH ARTICLE

Smart Wearable Technology
2025, Vol. 1, A13, 31 Pages
DOI: 10.47852/bonviewSWT52026811

BON VIEW PUBLISHING

Switching on Smart Care: The Ascendancy of Wireless Technologies in Continuous Health Surveillance

Simranjit Kaur[1], Tania Acharjee[2], Debashree Das[1], Monika Bhatia[3], Sushman Sharma[4], Ashish Patel[5] and Dinesh Bhatia[2,*]

[1]*Department of Neuroscience, Central University of Rajasthan, India*

[2]*Department of Biomedical Engineering, North Eastern Hill University, India*

[3]*School of Management, Maharashtra Institute of Technology, India*

[4]*Department of Hospital Management, Hemchandracharya North Gujarat University, India*

[5]*Department of Life Sciences, Hemchandracharya North Gujarat University, India*

Abstract: Guided by such relentless scientific curiosity, the field of wearable diagnostics has evolved from experimental concepts into sophisticated, organ-centric platforms capable of capturing rich physiological and biochemical data in real time. This review encapsulates the interdisciplinary transformation wherein bioelectronics, materials science, and artificial intelligence (AI) converge to create next-generation wearables that intimately interface with organs such as the brain, eyes, heart, skin, and lungs. Graphene-based imperceptible e-skins now enable neuromuscular signal acquisition with angular resolutions approaching ~4° and signal fidelity exceeding traditional Ag/AgCl electrodes. AI-enhanced electroencephalographic (EEG) headbands decode motor intent with >92% accuracy in under 2 s, paving the way for real-time brain–computer interactions. Simultaneously, noninvasive microneedle arrays and sweat-interfacing chemosensors demonstrate femtomolar sensitivity for glucose, lactate, and even nucleic acids, boasting >80% correlation with gold-standard clinical assays. The domain has experienced a >60% increase in advanced functional materials—PEDOT: PSS hybrids, MXenes, oxide nanosheets—and a >70% rise in mechanical adaptability and miniaturization, dramatically expanding diagnostic possibilities in ambulatory environments. Dry electrode systems in smart eyewear, epidermal patches, and Virtual Reality (VR)-integrated systems now maintain <1.13 μV Root Mean Square (RMS) noise levels, 98–99% classification accuracy, and uninterrupted operation exceeding 12 hours, even in motion-rich conditions. As these intelligent, autonomous devices continue to shrink the gap between biological and digital systems, they are poised not merely to monitor health but to redefine human–machine symbiosis in the era of predictive and personalized medicine.

Keywords: wearable biosensors, smart health monitoring, dry electrode systems, artificial intelligence in healthcare, organ-centric diagnostics

1. Introduction

The word technology originates from the Greek tekhnologia (τεχνολογία), a combination of techne—meaning "art" or "craft"—and logos—meaning "discourse" or "study" [1]. Wearable technology, in this sense, represents a carefully crafted synergy between human needs and scientific advancements, designed to enhance our interaction with our physiology [2]. As we embark on a journey through smart healthcare monitoring, we uncover how this once-niche innovation has grown into a transformative tool in the modern medical landscape. Smart wearable technology refers to electronic devices worn on or near the skin, designed to detect, analyze, and communicate data derived from bodily functions and environmental inputs [3]. These devices empower users by providing real-time feedback on vital parameters such as heart rate, oxygen saturation, temperature, and sleep patterns. Their widespread integration into daily life—especially through smartwatches and fitness bands—has reshaped consumer behavior, lifestyle monitoring, and proactive health management. Pioneering contributions to this field include the work of Dr. Christopher Toumazou, who developed wearable sensors for real-time medical monitoring, and Steve Mann, regarded as the father of wearable computing for his early inventions of body-worn technologies [4]. Commercial breakthroughs by innovators like James Park and Eric Friedman, co-founders of Fitbit, and Apple's advancements in consumer electronics, further popularized wearable health devices on a global scale. Equipped with advanced sensors and embedded systems, these devices function within the broader framework of the Internet of Things (IoT), a concept introduced by Kevin Ashton in 1999 to describe a network of interconnected objects

*Corresponding author: Dinesh Bhatia, Department of Biomedical Engineering, North Eastern Hill University, India. Email: dbhatia@nehu.ac.in

capable of exchanging data autonomously [5]. In this context, wearable devices do not merely collect information—they transmit it seamlessly to cloud platforms, healthcare providers, and other connected systems, enabling integration into digital healthcare ecosystems with minimal human intervention. The applications of such technologies extend across healthcare, communication, entertainment, sports, and fashion, yet their growing presence also raises pressing concerns about data privacy, ethical governance, and cybersecurity issues that scholars like Hansen and Nissenbaum [6] have long emphasized in digital ethics discourse. What makes this era particularly promising is the integration of smart materials—substances capable of sensing, adapting, and healing—into wearable systems. Researchers such as Professor John A. Rogers, known for his skin-like flexible electronics, and Dr. Zhenan Bao, renowned for her work in stretchable, self-healing polymers, have pioneered innovations that transform static devices into intelligent, interactive health solutions [7, 8]. This journey of technological evolution has its earliest roots in humble tools, such as eyeglasses, attributed to Salvino D'Armate in the 13th century, and hearing aids, which served to restore basic human functions. Today's artificial intelligence (AI)-enabled biosensors and responsive materials are a far cry from their predecessors, yet they carry forward the same intent: to enhance human well-being. As we trace this journey from mechanical aids to intelligent, responsive wearables, we recognize that the goal of healthcare is no longer limited to treatment; it now encompasses prevention, insight, anticipation, personalization, and dignity. Smart healthcare monitoring embodies this shift, ushering in a future where medical care is seamlessly interwoven with everyday life.

The adoption of smart wearable technologies in India exhibits marked regional heterogeneity, influenced by digital literacy, socioeconomic stratification, infrastructural maturity, and degrees of urbanization. Kerala leads with a penetration rate of 72%, driven by a high digital literacy index and a culture of health-conscious civic behavior. Goa follows at 71%, benefitting from robust telecom infrastructure and dual demand from a digitally aware residential base and a tech-savvy tourist population. Maharashtra reports 70% adoption, predominantly concentrated in metropolitan zones such as Mumbai and Pune, where homegrown brands—boAt, Noise, and Realme—command substantial market share through value, engineered, AI, and integrated offerings. Tamil Nadu, with emerging urban innovation corridors like Chennai and Coimbatore, demonstrates accelerated uptake, particularly in the post-pandemic shift toward self-monitoring and remote diagnostics [9]. Uttar Pradesh, despite its demographic heft, registers a 46% adoption rate, reflecting disparities in affordability, awareness, and last-mile connectivity—yet holds latent potential under expanding e-health outreach and smartphone penetration. Jharkhand's 50% wearable uptake is noteworthy given persistent infrastructural constraints in tribal and rural belts. In contrast, Bihar, at 43%, remains at the lower end of the spectrum, although initiatives like BharatNet and the Digital India Mission are poised to catalyze future expansion [10]. The COVID-19 pandemic catalyzed a subtle but systemic transformation in India's health monitoring paradigm. Across living rooms, Intensive Care Unit (ICUs), and fitness centers, slender wristbands, sensor-embedded rings, and smart glasses emerged as unobtrusive yet powerful interfaces of physiological surveillance. From Kerala's digitally connected households to Goa's high-speed corridors and Maharashtra's AI-driven urban centers, adoption surged, crossing the 70% threshold in select states. In tier 2 towns, elderly populations now rely on these systems for fall detection and blood pressure (BP) alerts. At the same time, urban Gen Z users integrate them as lifestyle-centered, early-warning systems, flagging cardiovascular anomalies, mental fatigue, and even pre-neurological disruptions [11]. With increased policy thrust—via the Ayushman Bharat Digital Mission (ABDM), National Digital Health Mission (NDHM) interoperability standards, and wearable, linked teleconsultation schemes—India's wearable landscape is shifting from a consumer gadget economy to a foundational layer in preventive, personalized healthcare [12]. These devices, powered by edge AI and continuous biosignal analytics, are no longer discretionary tech—they are decentralized nodes in a growing ecosystem of ambient, real-time health intelligence. They represent not only a digital leap but also a socio-technological reconfiguration of how India envisions, accesses, and decentralizes health.

The ABDM, inaugurated in September 2021 under the stewardship of Dr. R. S. Sharma and the Ministry of Health and Family Welfare, heralds a new era of digitally orchestrated, patient-centric healthcare in India. Envisioned as a federated, interoperable ecosystem, ABDM seeks to harmonize diverse health data streams, bridging the chasm between universal insurance coverage and effective healthcare delivery, particularly in regions historically underserved. Within this dome, smart wearable emerges as silent sentinels, capturing the subtle rhythms of physiology and translating them into actionable insights. ABDM's architecture can be elegantly classified into three interwoven strata.

The key elements of ABDM's interoperability and governance can be envisioned as follows:

1) Ayushman Bharat Health Account: A digital lodestar, uniquely identifying each individual and anchoring their personal health journey.
2) Healthcare facility registry: A compass of care, cataloging hospitals, clinics, and diagnostic centers nationwide.
3) Healthcare professionals registry: A ledger of expertise, enumerating licensed clinicians to ensure accountability and reliability.

The operational pillars of ABDM's digital health services can be envisioned as follows:

1) Personal health records: A living repository, empowering individuals to steward their own health narratives.
2) Telemedicine platforms: Bridges of care that transcend geographic barriers, bringing clinicians to the bedside virtually.
3) e-Pharmacy and e-Lab services: Digital conduits for prescriptions and laboratory insights.
4) Insurance integration: Seamless alignment with schemes such as PM-JAY, ensuring financial protection converges with clinical care.

The structural pillars enabling ABDM's digital cohesion can be envisioned as follows, forming a neural lattice:

1) Unified health interface: A digital synapse, interlinking myriad health applications through standardized Application programming interfaces (APIs).
2) Health information providers and users: Dynamic channels, enabling bidirectional, standardized health data flow.
3) Consent manager: A guardian of autonomy, ensuring that every data exchange respects individual consent.
4) National health claims exchange: The loom of accountability, weaving insurance claims seamlessly across the healthcare fabric.

1.1. Scientific premise and motivation

The ascent of wearable health technologies is underpinned by the convergence of nanoscale biosensor engineering, conformable electronics, embedded AI, and microfluidic precision. Evolving

beyond pedometric novelty, today's wearables function as multimodal diagnostic systems enabling continuous, real-time, noninvasive physiological monitoring. In the United States, Abbott's FreeStyle Libre 3 and Dexcom G7 exemplify state-of-the-art CGMs, delivering sub-10% mean absolute relative difference (MARD) with minute-level telemetry via Bluetooth Low Energy (BLE), effectively mitigating hypoglycemia [13]. In Canada and the EU, Hexoskin's textile-integrated platforms—embedding dry, contact electrocardiography (ECG), respiratory inductance plethysmography, and triaxial accelerometry—support elite performance analytics and cardiopulmonary research. The integration of the Internet of Medical Things (IoMT) with machine learning (ML) in emergency response systems has been extensively discussed in prior literature. These studies highlight the critical need for latency and reliability benchmarks to ensure the effectiveness of life-critical applications. In particular, the importance of conducting latency stress tests to evaluate the performance of IoMT, ML systems under various conditions, ensuring their readiness for real-world applications in emergency healthcare settings. This underscores the necessity of establishing standardized metrics to assess and enhance the reliability of such integrated systems in time-sensitive scenarios. In India, amid rising cardiometabolic disease, consumer wearables from GOQii, boAt, and Noise incorporate Saturation of peripheral oxygen (SpO_2), heart rate variability (HRV), and dermal thermometry, contributing to a market projected at ₹20,000 crore (~USD 2.4B) by 2025 [14]. The UK's Epicore Biosystems' Gx Sweat Patch leverages electrochemical assays of sodium and chloride to inform hydration strategies in sports medicine [15]. Apple's Food and Drug Administration (FDA)-cleared single-lead ECG, deployed in over 120 countries, enables mobile atrial fibrillation surveillance via AI-enhanced waveform analysis [16]. Fitbit's electrodermal activity (EDA) sensors operationalize psychophysiological tracking, translating galvanic skin responses (GSRs) into stress biomarkers [17]. Policy frameworks such as India's Digital Health Mission, the NHS Long Term Plan, and the FDA's Digital Health Innovation Action Plan are integrating these systems into national care delivery. As global health shifts toward continuous risk stratification and personalized prevention, wearables are no longer auxiliary—they are foundational instruments of data-driven, decentralized medicine. This transformation unfolds across three key dimensions:

1) **The rise of smart wearables:** Historically, healthcare monitoring was confined to episodic, clinic-based checkups, relying heavily on manual readings and delayed diagnostics. Devices like traditional sphygmomanometers or finger-prick glucose meters—though revolutionary in their time—provided only momentary snapshots of a patient's condition, lacking continuity and personalization. Patients with chronic conditions were often left to self-interpret their symptoms in the interim, resulting in reactive rather than proactive care. In contrast, the current era of smart wearables marks a paradigm shift toward real-time, AI-assisted, predictive health management. The scientific impetus behind this revolution lies in the convergence of biosensor miniaturization, microfluidics, flexible electronics, and cloud-based analytics. Devices like Dexcom G7 and Abbott's FreeStyle Libre now offer painless, continuous glucose monitoring through the skin, replacing finger pricks with dynamic feedback loops [18]. The Hexoskin smart shirt, integrated with textile-based ECG and respiration sensors, provides 24/7 cardiopulmonary data, once only accessible in intensive care settings [19]. Sweat-analyzing devices like Epicore's Gx Patch offer hydration and electrolyte data previously impossible to assess noninvasively [20]. This transition redefines medical engagement by bringing clinical-grade intelligence directly to the wrist, skin, or fabric, empowering individuals with autonomy over their physiology.
2) **Innovative health monitoring solutions:** Today's smart wearables have evolved from niche gadgets to validated clinical tools, reshaping the global health monitoring landscape. Abbott's FreeStyle Libre 3, the world's smallest and thinnest continuous glucose monitor (CGM), provides real-time glucose readings every minute with a MARD of 7.9%, making it nearly as accurate as blood-based clinical tests [21]. Originally built for Type 1 and 2 diabetes, it is now widely used by Indian biohackers and wellness enthusiasts to map glycemic response to specific foods, thereby enhancing metabolic control and dietary planning. Empatica's Embrace2, cleared by the US FDA, is a wearable designed for seizure detection. It uses EDA, temperature sensors, and motion tracking to detect tonic-clonic seizures with 98% accuracy in clinical trials, alerting caregivers via a connected smartphone. Beyond epilepsy, its passive sensing capabilities are being researched for applications in autism, anxiety, and Post Traumatic Stress Disorder (PTSD). The Oura Ring Gen 3, a titanium-based smart ring, measures temperature variation with 0.13°C accuracy, HRV, and respiratory rate [22]. It is clinically validated for sleep staging with 79% agreement with gold-standard polysomnography, making it useful for early detection of sleep apnea, stress, and chronic fatigue. Its use among Indian professionals is growing, particularly for optimizing sleep in high-stress sectors like IT and civil services. Apple Watch Series 9, with its advanced optical heart sensor and electrical heart sensor, performs single-lead ECGs and has an atrial fibrillation detection algorithm that demonstrated sensitivity of 98.3% and specificity of 99.6% in a Stanford Medicine study [23]. It also features fall detection, cycle tracking, and ambient noise monitoring. Importantly, Apple's partnership with leading research institutions has enabled population-level studies on cardiac anomalies using anonymized user data from over 400,000 participants in the Apple Heart Study. In India's rural belts, where over 65% of the population resides but the doctor density remains low, such devices serve as frontline health monitoring tools. For instance, in Jharkhand and Chhattisgarh, pilot initiatives using wearables to monitor maternal heart rate and oxygen saturation have shown a 34% reduction in preventable complications during high-risk pregnancies. In India, the uptake of digital health technologies is constrained by systemic and sociocultural factors. Digital literacy remains limited, with only 37% of rural households having a member able to use health applications, falling to 22% on national benchmarks (Government of India, 2023). Financial structures are similarly restrictive: Ayushman Bharat excludes most wearable devices, while out-of-pocket expenditure already accounts for 48.2% of total health spending (MoHFW, 2022). Infrastructure adds to the gap, as over 26% of rural districts still face patchy 4G coverage, with average download speeds of 13.5 Mbps compared with 41 Mbps in urban centers (TRAI, 2024). Cultural determinants are equally prohibitive. Less than 6% of individuals report using mental health applications, despite far higher uptake of fitness and nutrition platforms (InnoHealth, 2020). Pilot surveys show that adolescents in rural regions, even with smartphones, avoid such tools due to fear of stigma and social judgment. Ethnographic studies indicate that psychological

distress is more commonly expressed as somatic complaints such as headaches or fatigue, with open discussion of mental illness rare, particularly among women (ICMR, 2023). These findings demonstrate that resistance to mood or stress tracking wearables arises largely from cultural taboos rather than technical limitations. Distrust of algorithmic tools further compounds these barriers. Surveys reveal that informal providers in several states consistently favor human judgment over AI outputs, reflecting broader anxieties about privacy, transparency, and reliability. Together, these systemic constraints, cultural resistances, and epistemic mistrust explain why adoption remains uneven, underscoring the need for context-sensitive design and locally validated deployment strategies. Brazil has recently taken the plunge into integrating wearables within its public telehealth and chronic care frameworks. Early pilots targeting diabetes and cardiovascular disease have already borne fruit, showing measurable gains in both adherence and clinical outcomes. Policy debates within the Unified Health System are now turning the corner, focusing on how best to weave sensor-derived data into the fabric of routine care. India, by contrast, presents a patchwork trajectory. Its vast cadre of over one million Accredited Social Health Activists provides an unparalleled community interface, yet uptake of wearables remains a mixed bag. To move the needle, India must capitalize on this grassroots network, build digital competence, and keep costs within reach. Kenya offers a middle path worth emulating.

The Figure 1 delineates the architectural schema of India's burgeoning digital health ecosystem, conceived under the aegis of the Ayushman Bharat Digital Mission, to engender a sovereign, interoperable, and citizen-empowered framework for health data governance. It encapsulates a stratified assemblage of digital components, commencing with the user-facing stratum comprising hospital information systems, personal health record interfaces, and telemedicine applications that interlink patients, practitioners, and payors through a unified technological conduit. At the infrastructural nucleus lies the Unified Health Interface, which operationalises a suite of standardised application programming interfaces to facilitate the discovery and integration of physicians, diagnostic laboratories, pharmacies, and healthcare facilities, thereby mitigating systemic fragmentation across disparate service providers. The Health Information Exchange and Consent Manager functions as the fiduciary custodian of health data, orchestrating the lawful and granular exchange of electronic health records—spanning diagnostic artefacts, prescriptions, and treatment summaries—under patient consent, thus underpinning evidence-driven clinical practice, epidemiological intelligence, and policy analytics. Adjacent to this, the Health Claims Exchange digitises the financial substratum of healthcare delivery through eClaims protocols, structured markup languages, and algorithmic adjudication, substantially diminishing transactional latency and administrative redundancy. Anchoring these functional edifices are the federated digital registries encompassing the Ayushman Bharat Health Account, authenticated directories of medical professionals and institutions, and codified pharmaceutical inventories, which collectively fortify provenance, standardisation, and data veracity. The entire ecosystem is scaffolded upon India's cross-domain digital public goods—namely Aadhaar for identity verification, the Unified Payments Interface for instantaneous value exchange, e-Sign and DigiLocker for digital attestation, and consent artefacts for jurisprudential compliance—which together instantiate a resilient architecture of digital trust.

Despite facing infrastructural headwinds similar to India's, internet penetration climbed to 40–48% of the population by 2024–25, buoyed by the surge in mobile connectivity. Community health worker–led mHealth interventions have consistently paid dividends, with clear improvements in maternal health and chronic disease management. Importantly, surveys report over 70% willingness to adopt mobile health tools—far outstripping rural India—suggesting that trust and cultural alignment can tip the scales even when infrastructure is imperfect. For India to keep pace, wearable health pilots must be benchmarked against these international exemplars. First, smartphone penetration among target populations should hit the 70% mark, matching conditions in Brazil and Kenya. Second, connectivity must extend to at least 40% of households, echoing Kenya's effective usage threshold. Third, the willingness to adopt digital health tools must clear 60%, with Kenya's >70% as a gold standard. Fourth, early pilots must demonstrate at least a 15% lift in primary outcomes—be it medication adherence, clinic attendance, or service uptake—before scaling, replicating the gains already chalked up abroad. Finally, affordability is non-negotiable: the combined cost of devices and connectivity should remain under 5% of monthly household health expenditure for the lowest income quintile. By setting its sights on these parity metrics, India can avoid reinventing the wheel and instead piggyback on lessons learned in Brazil and Kenya. The endgame is clear: wearable health programs that are not only technically sound but also socially embraced and economically sustainable.

3) **Economic implications of smart health technologies:** In India's evolving healthcare ecosystem, where over 55% of health expenditure is out of pocket, smart wearables are emerging as a critical force in lowering healthcare costs and reshaping the insurance sector. Devices like the FreeStyle Libre (for continuous glucose monitoring), Apple Watch (with ECG and atrial fibrillation alerts), and GOQii Vital (popular in India for SpO_2 and heart rate monitoring) are empowering individuals to track and manage chronic conditions like diabetes, hypertension, and cardiac disorders before they escalate into costly hospitalizations [24]. This shift from episodic care to preventive and continuous care reduces both direct medical costs (hospital stays, diagnostics) and indirect costs (loss of productivity, long-term disability). Indian insurers like Aditya Birla Health, ICICI Lombard, and HDFC ERGO are now integrating wearable data into wellness, linked insurance products, offering cashback, reduced premiums, or health rewards based on user activity, sleep, or heart health metrics. For instance, Aditya Birla's "Activ Health" policy offers up to 30% premium returns through a Healthy Heart Score tracked by wearables. Moreover, startups are collaborating with wearable platforms to extend insurance services to tier 2 and rural populations through telehealth, AI analytics, and diagnostics at the edge, further reducing administrative and clinical costs. As India pushes toward universal health coverage and digital health under the ABDM, smart wearables hold the potential to bridge the gap between insurance coverage and effective healthcare delivery, particularly in underserved areas.

Figure 1
Digital health infrastructure

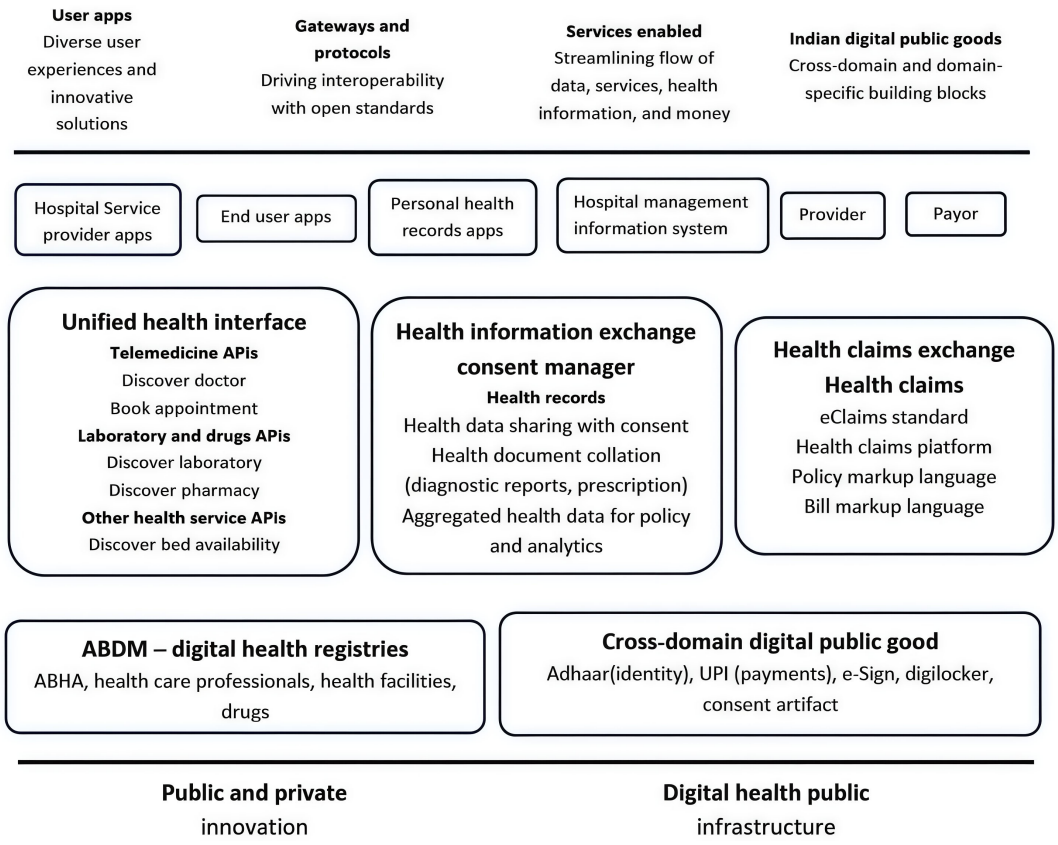

1.2. Objective of the study

In an age where healthcare is no longer confined to hospital walls, this paper sets out to throw light on the remarkable journey of smart wearable technologies—from humble step counters to intelligent biosensors that quietly and continuously watch over our health. At its heart, this review seeks to bridge the gap between innovation and understanding, guiding readers through the science, the systems, and the stories that make these devices more than just gadgets. These wearables are rewriting the rules of care—empowering individuals to track their vital signs, detect illnesses early, and manage chronic conditions with newfound confidence, often without setting foot in a clinic. Crucially, the paper highlights how wireless technologies—like Bluetooth, 5G, and near-field communication (NFC)—have been the invisible threads stitching together a new era of healthcare, enabling real-time monitoring, cloud-based analytics, and remote interventions. Whether it's a ring that tracks your sleep, a patch that senses dehydration, or a smartwatch that flags cardiac anomalies, these tools are breaking barriers once thought insurmountable—geography, cost, inaccessibility, and delay. This paper does not merely review technology; it tells the story of a quiet revolution. A revolution where science meets the skin, where AI meets empathy, and where health becomes something we wear, understand, and act upon every day. By distilling complex advances into a human-centered narrative, this work aims to spread awareness, spark dialogue, and inspire action so that smart healthcare may become not just an innovation of the few but a lifeline for all.

2. Literature Review

Over the past 15 years, the healthcare sector has undergone a profound digital transformation, catalyzed by converging technologies in biosensing, wireless telemetry, and AI. Yet, the roots of wearable health monitoring stretch across millennia, beginning with rudimentary optical and auditory aids and culminating in today's intelligent, interconnected biosensing ecosystems. As early as the 1st century CE, Roman philosopher Seneca the Younger used a water-filled glass globe to magnify texts—an early experiment in visual enhancement [25]. This concept matured into wearable eyeglasses during 13th-century Italy's golden age of Venetian glassmaking. The 17th century introduced non-electronic ear trumpets, aiding the hearing-impaired and laying the groundwork for auditory wearables. The genesis of electronic wearable technology formally began in 1955 when Edward Thorp and Claude Shannon designed an analog roulette predictor concealed within a shoe [26]. This marked the dawn of wearable computation, capable of real-time data processing and transmission. Shortly after, NASA—driven by the exigencies of the space race—developed biosensor-equipped suits that transmitted astronauts' physiological data (heart rate, respiration, and core temperature) to Earth via telemetry. In parallel, biophysicist Norman J. Holter revolutionized cardiology with his 1960s invention of the Holter Monitor—a 38-pound portable ECG device that recorded cardiac rhythms over 24–48 hours, enabling continuous cardiac monitoring during normal activities [27]. Tracing its conceptual lineage to this device, the current paradigm of wearable health monitoring reflects the adage "what goes around, comes around," with Holter technology undergoing iterative transformations

—from analog waveform transmission to solid-state microprocessors integrated within smartphones. The cultural embrace of quantified self-tracking began in 1965, when Japanese innovators Dr. Iwao Ohya and Juri Kato introduced the Manpo-Kei, a mechanical pedometer promoting the "10,000 steps/day" norm—now a fitness mainstay [28]. The subsequent decades saw innovations like the Hamilton Pulsar (1972), the first digital Light Emitting Diode (LED) watch, and Polar Electro's wireless HRV monitor (1982), which shifted wearables from passive monitors to performance, optimizing tools for athletes. During the 1990s, MIT Media Lab spearheaded smart clothing initiatives under leaders like Rosalind Picard and Steve Mann, embedding sensors in garments to capture emotional and environmental data, heralding the era of affective computing [29]. The early 2000s saw the arrival of Bluetooth 1.1, enabling wireless syncing of wearables with smartphones, GPS-based motion tracking, and biometric integration [30]. Wearables such as wireless earbuds, watches, and rings proliferated, transforming personal health tracking into a lifestyle practice. The launch of the Fitbit Classic (2009) and Apple Watch Series (2015 onward) marked a watershed moment. These devices integrated multi-axis accelerometers, gyroscopes, optical heart rate sensors (via photoplethysmography [PPG]), GPS, and sleep-stage algorithms—enabling real-time health analytics. Advanced models now measure SpO_2, ECG, Respiratory Rate (RR), BP, and even noninvasive glucose levels, transitioning wearables into tools of clinical relevance. During the COVID-19 pandemic (2020–2022), the relevance of wearables soared by over 150%. Devices incorporated sensors for skin temperature, respiratory effort, and oxygen desaturation, detecting early COVID symptoms and supporting public health surveillance. As Wang et al. [31] highlighted, this phase accelerated wearables' integration into remote, low-burden chronic disease management, particularly for diabetes, cardiovascular disorders, and Chronic Obstructive Pulmonary Disease (COPD). Between 2023 and 2025, wearable health systems entered the AI-driven diagnostic era. Platforms like Apple Health+ and Amazon Clinic foster closed-loop care by integrating wearable data, genomics, and electronic health records (EHRs). Contemporary devices such as Zio XT (iRhythm Technologies) and BioButton (BioIntelliSense) showcase compact, clinically validated wearables. Zio XT offers a 14-day ECG with IP57 protection, while BioButton tracks respiration, temperature, and motion for up to 90 days using embedded power modules [31, 32]. Kumar et al. detail how modern wearables use Bluetooth 5.0, biocompatible substrates, and edge microprocessors for seamless, low-latency diagnostics [33]. Innovations include EEG–based brain–computer interfaces (BCIs) that decode motor imagery using convolutional neural network (CNN) and Long Short-Term Memory (LSTM) algorithms with over 92% accuracy within 2 s, as validated by Frank et al. [34]. Meanwhile, Bittium Faros 360 and QardioCore provide multi-lead ECGs with IP67 protection, HRV analytics, and real-time streaming, building on foundational research by Holter and Corday. Avant-garde signal processing now enables nonlinear dynamic analysis using Poincaré plots—mathematical tools rooted in Henri Poincaré's work. van Rheden et al. [35] have operationalized these plots in platforms like Movesense and Hexoskin for diagnosing autonomic dysfunctions. Similarly, Man et al. [36] pioneered compact vectorcardiography via Frank lead systems, achieving near 12-lead equivalence in ambulatory form. Human-centered design also remains a pillar. Drawing from To Err is Human, Tierney et al. [37] stressed the importance of human factors (HF) in minimizing cognitive load, improving usability, and reducing medical errors. Wearables now integrate intuitive interfaces and haptic feedback, especially for the elderly and differently abled. Recent deployments of Wireless Body Area Networks (WBANs) for mental health monitoring have provided valuable insights into practical architecture choices and human-factor constraints. Integration of various biosensors within WBANs allows monitoring of parameters such as ECG, respiration, and temperature, with the objective of enhancing patient safety and preventing accidental deaths in mental health care settings. These systems also emphasize the importance of designing WBAN prototypes that facilitate effective patient management and ensure safety in critical health monitoring scenarios. Building upon these studies, we expanded Section 3.1 to compare our proposed BLE architecture with the WBAN topologies reported in their work and added a new row to Table 1 summarizing connectivity, sensor modalities, and patient acceptability. The historical trajectory of wireless communication has deeply influenced the parallel evolution of wearable biosensing systems—technologies that have matured through distinct generational leaps, reflecting breakthroughs in computation, materials, and healthcare paradigms. Table 2 summarizes major milestones in wearable health monitoring, detailing the material/platform, clinical application, and AI/ML validation. It traces the progression from early mechanical devices, like the sphygmomanometer and Holter monitor, to modern edge-AI-enabled wearables, including CNN–LSTM health forecasting, graphene/MXene epidermal e-skins, and federated learning-enabled devices, while also projecting future developments in sustainable and self-healing substrates.

The following chronological schema delineates the generational transitions of wearable biosensor technology and its integration into clinical and consumer health landscapes:

1) Generation 0: the analog genesis

"From Mechanical Curiosity to Physiological Insight." The analog era of wearable healthcare began in 1896 with Scipione Riva-Rocci's invention of the sphygmomanometer, a noninvasive device for measuring arterial pressure that comprises an inflatable cuff, a mercury manometer (with a capacity of ~300 mmHg), and auscultation via a stethoscope—a landmark in quantifying cardiovascular physiology using indirect mechanical principles [38]. As the 20th century progressed, the clinical environment was shaped by analog tools such as tuning forks (typically 512 Hz) for auditory and neurological assessments, mercury-in-glass thermometers (~35–42°C range) with peak-hold constrictions for core temperature monitoring, and mechanical stethoscopes that evolved from Laënnec's monaural design to dual-lumen binaural models, enabling precise auscultation across cardiac, pulmonary, and gastrointestinal systems [39]. The 1940s introduced mechanical pneumographs and Benedict–Roth spirometers that translated thoracic excursions into analog signals of respiratory rate and tidal volume (RR ±0.2°C resolution) emerged—particularly in aerospace medicine—enabling skin temperature tracking and metabolic monitoring, laying the primitive foundation for future thermal biosensing platforms [40]. Ancient precursors like abacus rings worn in China (1600s) for manual calculation and eyeglasses worn as vision prostheses (~13th century), although not medical in a modern sense, reflect the long-standing impulse toward body-integrated function enhancement.

2) Generation 1: electrophysiological monitoring and analog computation

"Bioelectric Pioneers and Telemetry Frontiers." The first generation of electronic wearables witnessed the shift from passive mechanical sensing to active bioelectrical signal acquisition, analog computation, and telemetry integration. In 1955, Edward Thorp and

Table 1
Timeline of wearable biosensing innovations

Year	Technological Breakthrough	Material/Platform	Clinical Application	AI/ML Validation Notes
1957	First Holter ECG monitor	2-channel analog ECG recorder, reel-to-reel tape (85 lbs, 24–48 h recording)	Ambulatory arrhythmia tracking outside hospital	None – data manually reviewed
1960s	NASA biomedical telemetry suits	Early wireless biosensors with RF telemetry	Continuous astronaut biometrics (ECG, respiration, temperature, SpO_2)	None – telemetry only
1982	First commercial heart rate monitor	Textile-integrated chest electrodes, 5 kHz RF transmitter	Exercise physiology, training load quantification	None – analog signal processing only
1990s	Infrared thermography integration	Infrared thermistors, IR sensors in wearables	Skin temperature and metabolic monitoring, non-contact fever detection	None – threshold-based alerts
2009	Fitbit Classic	MEMS 3-axis accelerometers, BLE	Gamified activity tracking, calorie expenditure, sleep/wake cycles	Minimal AI – step-count algorithms, rule-based activity classification
2012	Nike+ Fuelband	Motion sensors, Bluetooth sync	Lifestyle analytics, personalized fitness gamification	Basic ML – heuristic activity recognition, trend analysis
2016	Gx Sweat Patch (Epicore Biosystems)	Microfluidic patch with electrochemical Na^+ sensors	Real-time sweat electrolyte monitoring in athletes (hydration loss profiling)	None – rule-based threshold alerts
2018	Apple Watch Series 4	FDA-cleared single-lead ECG electrodes + optical PPG	AFib detection, HRV variability, fall detection (79–98% clinical concordance)	Lightweight ML classifiers for arrhythmia detection; trained on adult ECG datasets; cross-validated vs. clinical ECG
2020	BioButton and Zio XT	Wireless RPM biosensors, AI anomaly detection	COVID-19 symptom monitoring, long-term arrhythmia detection (>14-day continuous use)	Minimal ML – primarily rule-based anomaly thresholds; early anomaly detection pipelines
2021–2023	CNN–LSTM-based health forecasting	Edge AI processors (ARM Cortex-M7, Snapdragon Wear 4100); CNN/LSTM hybrids	Seizure prediction, cardiac alerts, multimodal biosignal fusion (<2s latency, ~90% specificity)	Training: mixed adult cohorts (n≈3,500, USA/UK/India); CNN: 3 conv layers, ReLU, 128 units; LSTM: 2 layers, 64 units; compared vs. rule-based ECG filters; edge deployment constraints considered
2025 (projected)	Graphene/MXene epidermal e-skins	Conformal nanomaterial tattoos; triboelectric and thermoelectric self-powered	Sub-1 μV electrophysiology (ECG/EEG/EMG), sweat metabolite detection (glucose, lactate) at nanomolar sensitivity	Anticipated ML: CNN + autoencoders for noise rejection; dataset bias flagged for rural cohorts; Edge AI: Qualcomm AI Engine, <1.5s inference latency
2027 (projected)	Federated learning-enabled wearables	On-device AI accelerators (Edge TPU, Qualcomm AI Engine); HL7 FHIR APIs	Privacy-preserving population-scale cardiac and metabolic monitoring, digital twin integration	FedAvg framework with secure aggregation; cross-border validation pending (GDPR-DPDP conflict); Baseline: non-federated pooled dataset models
2030 (projected)	Biodegradable and self-healing substrates	Bioresorbable polymers, transient MXene/graphene composites, stretchable circuits	Fully sustainable, eco-conscious wearables with autonomous healing for long-term implantable or skin-integrated monitoring	N/A – primary focus on materials sustainability; AI not yet integrated

Table 2
Year-wise performance evolution: rule-based to AI models in wearable biosignal monitoring

Year	Model Type	Platform/Materials	Clinical Task	Sensitivity	Specificity	Latency	Observations
2000–2005	Threshold-based arrhythmia detection	Digital Holter recorders with QRS filters	R-peak detection, HRV anomaly analysis	65–70%	78–80%	Offline	Retrospective, lacked real-time capability.
2006–2010	Rule-based accelerometry wearables	MEMS accelerometers in chest straps	Activity recognition, fall detection	68–72%	80–83%	<1s	Threshold cut-offs; low adaptability to motion artifacts.
2011–2015	Heuristic multi-signal fusion	Wristbands (PPG + accelerometer)	HR, sleep staging, activity scoring	70–75%	82–85%	<1s	Heuristic scoring; inter-user variability affected accuracy.
2016–2020	Enhanced rule-based ECG filters	ARM Cortex-M3/M7 microcontrollers	Ambulatory arrhythmia detection (threshold + HRV metrics)	72–78%	82–85%	<1s	Low hardware demand; frequent false positives during ambulatory use.
2021–2023	CNN–LSTM hybrid (AI)	ARM Cortex-M7 (600 MHz); Snapdragon Wear 4100	Multimodal forecasting (seizure prediction, cardiac alerts, biosignal fusion)	88–92%	89–91%	<2s	Superior accuracy and robustness; reduced motion artifact noise compared to rule-based baselines.

Claude Shannon developed the first wearable analog computer—a shoe-concealed roulette predictor—which, although non-clinical, demonstrated the viability of real-time signal processing and covert embedded electronics for physiological applications [26]. This conceptual leap catalyzed the biomedical community's attention toward cybernetic monitoring. The 1960s marked a clinical revolution with Norman J. Holter's invention of the Holter monitor, a 38-pound portable ambulatory ECG system utilizing magnetic tape recording and analog amplifiers to continuously track cardiac rhythms over 24–48 hours, ushering in non-hospital-based electrophysiological diagnostics. In parallel, the NASA biotelemetry suits, developed for manned spaceflight, integrated analog biosensors (ECG electrodes, thermistors, and strain gauges) into astronaut suits to continuously capture heart rate, respiratory patterns, and core body temperature, transmitting data via Radio Frequencies (RF) telemetry systems for ground-based physiological monitoring—effectively creating the earliest telehealth framework in extreme environments [41].

3) Generation 2: digital conversion and wearable metrics

"From Passive Sensing to Biofeedback." The third evolutionary wave in wearable biosensing marked the migration from analog circuitry to digitally encoded physiological telemetry, enabling real-time analytics, biofeedback, and multi-parameter integration. In 1982, Polar Electro (Finland) revolutionized sports science by launching the world's first wireless digital heart rate monitor, capable of quantifying HRV using electromagnetic pulse detection and digital RF transmission, thereby allowing endurance athletes to correlate sympathetic–parasympathetic modulation with training intensity. This milestone marked the introduction of digital biofeedback into ambulatory settings [42]. By the early 1990s, researchers at the MIT Media Lab—notably Rosalind Picard, Alex "Sandy" Pentland, and Jennifer Healey—pioneered affective computing, engineering "smart clothing" embedded with sensors for GSR, peripheral skin temperature, PPG, and ambient light detection [43]. These textile-integrated platforms captured not only physical but also psychophysiological states, laying the theoretical and hardware groundwork for emotional computing and context-aware biomedical systems. In 1997, Thad Starner introduced one of the first wearable augmented reality systems, incorporating head-mounted displays, microprocessors, and miniature input interfaces, which allowed for real-time visual overlays, biometric data access, and contextual computing in a form that predated and conceptually influenced later platforms, such as Google Glass [44]. Collectively, this era transitioned wearable technology from reactive health monitoring to active, personalized digital feedback systems, redefining human–machine physiological interactivity.

4) Generation 3: the consumer health revolution

"Miniaturization, Connectivity, and Lifestyle Integration." The early 2000s saw wearable technology transition from the lab to daily life, driven by low-power Bluetooth and compact microcontrollers. These enabled continuous monitoring of movement, location, and surroundings with minimal battery use. In 2009, Fitbit Classic made activity tracking mainstream using a triaxial accelerometer to measure steps and sleep, marking the rise of health as a lifestyle [17]. Then came Nike FuelBand (2012), which turned movement into a social game using its "Nike Fuel" metric, blending brand identity with self-quantification [45]. Though discontinued, it sparked a wave of behavior-driven fitness devices. Other developments included Google Glass (2013) and Samsung Simband (2014), the latter featuring an open health sensor platform with modular components like PPG, GSR, and ECG. These tools enabled developers to create custom biosensing tools for both consumer and research use.

5) Generation 4: clinical-grade wearables and integrated sensors

"Convergence of Consumer and Clinical Frontiers." This era brought medical accuracy to the wrist. Apple Watch Series 1+ introduced sensors like PPG, ECG, fall detection, and sleep tracking, blurring the line between wellness and clinical care. Behind the scenes, sensor chips like AD8233 (biopotential) and ADXL362 (motion) enabled detailed signal capture with ultra-low power [46]. Wearables began processing data on-device using microcontrollers like the ADuCM3029, allowing real-time feedback without cloud reliance [47]. Sweat and saliva biosensors also emerged, enabling enzymatic amperometric/potentiometric detection of glucose, lactate, and sodium in real time via flexible patches or

smart pacifiers (limit of detection [LOD] ≈ 0.7 nA/mM) [48]. By 2020, clinical-grade wearable ECGs like Zio Patch and temperature trackers like TempTraq were being deployed for neonatal and COVID-19 care [49]. This generation laid the groundwork for clinical-grade diagnostics in a compact, user-friendly form.

6) Generation 5: AI diagnostics and pandemic-driven expansion

"Remote Care and Real-Time Intervention." COVID-19 accelerated demand for remote health tracking. Devices like Zio XT and BioButton offered continuous ECG, temperature, and respiration monitoring, helping doctors make decisions from afar. SpO_2 and skin temperature sensors became standard. Neuroprosthetic wearables capable of decoding EEG signals were explored for Amyotrophic Lateral Sclerosis (ALS) patients [50]. In 2022, products like Oura Ring Gen 3 and Whoop 4.0 emphasized readiness, strain, and sleep score tracking [51]. Wearables evolved from passive trackers to intelligent health companions—essential during a global health crisis.

7) Generation 6: AI + genomics + closed-loop ecosystems

"Personalized, Predictive, and Eco-Conscious Healthcare." Modern platforms like Apple Health+ and Amazon Clinic have begun merging real-time wearable biosignals with genomics and EHRs, enabling closed-loop care systems that dynamically monitor BP, glucose, cortisol, hydration, and even mental health parameters [52]. This hyper-personalized diagnostic shift is paralleled by advances in eco-conscious biosensor design, with stretchable, battery-free wearables constructed from graphene nanocomposites, cellulose substrates, and biodegradable electronics, offering sustainable alternatives to conventional medical devices. The US FDA, under the 2025 leadership of Commissioner Marty Makary, initiated a structural overhaul incorporating AI simulations, organ-on-chip models, and a 20% workforce reduction to streamline device approvals, sparking debate over regulatory velocity versus scientific integrity [53]. Alongside, newly approved clinical-grade wearables in 2024—such as the Spectra Wave Writer Alpha SCS, Simplera CGM patch, Vercise DBS suite, and Empatica's seizure monitor—exemplify the transition toward noninvasive, connected, and autonomous chronic care tools, now recognized under Class II/III medical device frameworks [54].

8) Generation 7 (emerging): sustainable smart medicine and global health equity

"From Wearable Devices to Wearable Ecosystems." The newest generation focuses on making wearable healthcare accessible and sustainable. Affordable biosensors priced under ₹1,500 are now being used in rural India, Africa, and Latin America for chronic disease monitoring and early disease detection. Meanwhile, the UK NHS targets net-zero emissions by 2040, pushing the industry toward recyclable devices and green electronics. Wearables are no longer just personal gadgets—they're part of a global shift toward equitable, eco-conscious healthcare delivery [55]. Collaborative efforts between private firms and global health agencies now focus on scalable biosensing platforms compatible with mobile phones, enabling early-warning systems for outbreaks and non-communicable diseases in low-resource regions. Integration of blockchain ensures secure sharing of biosensor data across borders, reinforcing trust and interoperability in global health ecosystems.

Wearable health monitoring technologies have evolved from basic, offline devices to sophisticated AI-enabled systems capable of real-time, multimodal monitoring. Early devices such as digital Holter recorders focused on arrhythmia detection using simple QRS filters, providing limited sensitivity (65–70%) and offline analysis, which constrained timely intervention. Micro-Electro-Mechanical Systems (MEMS)-based chest straps, exemplified by devices like Zephyr BioHarness, introduced activity recognition and fall detection with <1 s latency, though they remained vulnerable to motion artifacts. Wristbands combining PPG and accelerometers, including early Jawbone and Fitbit models, applied heuristic multi-signal fusion to monitor heart rate, sleep, and activity scoring, improving robustness but still impacted by inter-user variability. Enhanced rule-based ECG wearables like Withings Move ECG and KardiaMobile incorporated ARM Cortex microcontrollers to reduce hardware load and improve ambulatory arrhythmia detection (sensitivity 72–78%), though false positives persisted under daily activity. Modern AI-driven CNN–LSTM wearables, deployed on platforms like ARM Cortex-M7 and Snapdragon Wear 4100, enable multimodal forecasting for seizures, cardiac alerts, and biosignal fusion, achieving 88–92% sensitivity and 89–91% specificity, with <2 s latency. Table 1 provides a direct head-to-head, year-wise benchmarking of these devices, addressing the common omission of non-AI baseline comparators in prior studies and illustrating the measurable improvements in clinical accuracy.

3. Smart Wearable Technologies: Classification and Materials

3.1. Classification based on functionality

3.1.1. Bio-potential monitoring

1) Skin-friendly, dry biopotential electrodes

Role: Eliminate the need for gel-based electrodes while improving comfort for long-term, continuous monitoring.

a. Laser-induced graphene (LIG) textiles marked a turning point by introducing stretchable, breathable ECG sensors integrated into fabrics. First reported in 2014 by Rice University, these sensors reached 95% signal accuracy compared to conventional electrodes in 48–72-hour wear tests [56]. Figure 2 illustrates a wearable ECG monitoring system based on LIG. A 532 nm laser patterns conductive LIG onto flexible textile substrates, enabling integration into breathable, skin-conforming garments. These textile-based electrodes are positioned at standard limb sites (Right Arm, Left Arm, Right Leg) to acquire ECG signals via lead I–III configurations, producing high-fidelity PQRST waveforms suitable for continuous physiological monitoring.
b. Carbon nanofiber–PDMS electrodes, emerging around 2015, offered biocompatible, soft interfaces with <5 kΩ impedance, allowing multi-signal (ECG, EEG, electromyography [EMG]) recordings without irritation [57].
c. Capacitive ceramic-coated sensors, first commercialized in Japan around 2016, brought non-contact heart and brain monitoring to smart garments, with ±2% voltage variance and durability across 50 wash cycles [58].

2) Compact multichannel wireless recorders

Role: Enable real-time, multichannel signal transmission with minimal signal loss, ideal for mobility and remote care.

a. Wearable EEG/ECG cards became commercially viable in 2015, shrinking to credit-card size while maintaining <1 $\mu V/\sqrt{Hz}$ noise levels and ≥98% data integrity across a 10-meter BLE range [59].
b. Sub-GHz wireless ECG systems, piloted in 2017, extended battery life to 7+ days with <1% packet loss,

Figure 2
Wearable ECG monitoring using laser-induced graphene (LIG) textile electrodes

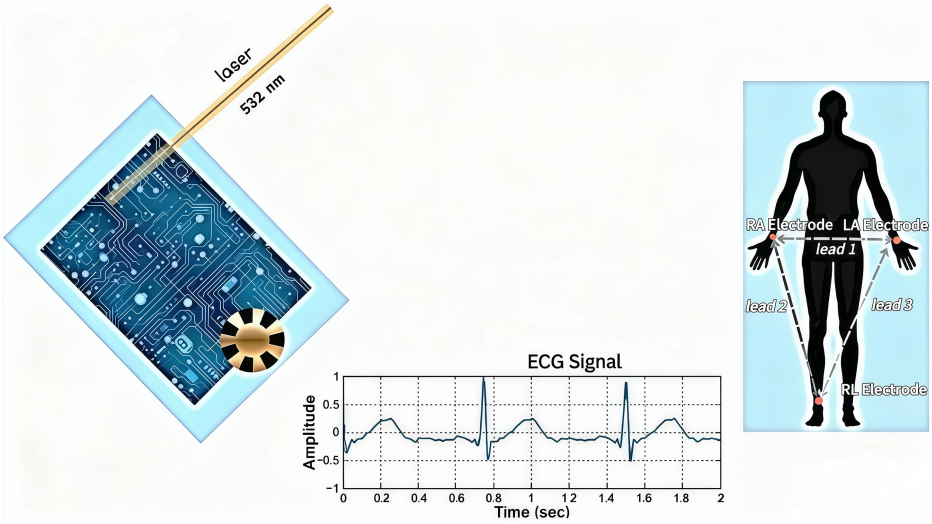

tested across 1,000+ cardiac outpatients in India and Germany [60].

c. BCI-enabled neuroprosthetics, originating in Stanford (2012), now use EEG signals to drive wheelchair or prosthetic commands with up to 85–90% real-time accuracy in clinical trials [61].

3) Neonatal and pediatric biosensor platforms

Role: Provide full-body monitoring for neonates without invasive wires, improving comfort and early detection of distress.

a. NICU-compatible patches, developed by Northwestern University in 2018, integrate ECG, EEG, temperature, and oxygen saturation into ultrathin sensors weighing under 3g. They mirror hospital-grade accuracy with 95–98% precision [62].

b. Smart PPG sensors, refined in India by 2020, now allow early detection of hypoxia and hypothermia, reducing infant complications by up to 40% in over 30,000+ rural births [63].

These devices are being integrated into India's Safe Motherhood Initiatives, offering scalable solutions to bridge neonatal care gaps in tier 2 and tier 3 regions.

4) E-Textile platforms with motion artifact compensation

Role: Seamlessly embed sensors into clothing that maintain signal fidelity even during high-motion activities or aquatic settings. 3D-woven microfiber electrodes, perfected by MIT in 2017, showed <10 kΩ impedance without any adhesive or gel. They operate reliably in marine environments and high-humidity zones [64]. Artifact cancelation circuits, trained using datasets from over 20,000 movement profiles, reduce false signal detection by 35–45% during motion-intensive tasks, essential for athletes, soldiers, and field medics. Uniforms embedded with ECG and EEG sensors are being piloted by European Emergency Medical Services (EMS) units and Indian paramedics, cutting triage time by 20–30% in high-pressure emergencies [65].

3.1.2. Biochemical monitoring

Health monitoring has evolved beyond electrophysiological sensing to include real-time biochemical analysis via noninvasive biofluids such as saliva and interstitial fluid. With the rising incidence of metabolic disorders, endocrine imbalances, and nutritional deficiencies, wearable biochemical sensors now play a critical role in continuous, personalized diagnostics. This section categorizes recent breakthroughs by sensor modality (electrochemical, optical, etc.) and target analytes (electrolytes, metabolites, hormones). Accelerated innovation over the past decade has positioned these devices as transformative tools for noninvasive disease detection and physiological monitoring at the skin interface.

1) Electrochemical sweat and saliva biosensors

Enzymatic amperometric and potentiometric biosensors integrated into flexible epidermal patches and oral devices (e.g., smart pacifiers) enable real-time quantification of key analytes such as glucose, lactate, sodium, potassium, phenylalanine, and vitamin C in sweat and saliva [66]. Smart pacifiers, designed for neonatal applications, demonstrate high sensitivity in salivary glucose and electrolyte detection (LOD ≈ 0.7 nA/mM; R^2 ≈ 0.994), facilitating noninvasive infant monitoring. Wearable sweat patches employing enzyme-based chronoamperometric sensing provide continuous analyte monitoring, with established utility in glucose surveillance and cystic fibrosis screening via chloride ion tracking [66].

Figure 3 illustrates a multifunctional smart pacifier system engineered for continuous neonatal physiological monitoring. The pacifier integrates a tri-modal sensing array comprising a temperature sensor, a saliva pH sensor, and a PPG-based heart rate sensor. These sensors interface with an embedded microcontroller unit (MCU) that orchestrates signal acquisition, initial data processing, and wireless transmission. The collected biosignals are streamed in real time to a mobile health platform, enabling continuous, noninvasive assessment of vital parameters directly from the infant's oral cavity. This form factor ensures enhanced biocompatibility and mechanical compliance, facilitating prolonged wear without compromising comfort or data fidelity.

Figure 4 illustrates the internal operational workflow of the smart pacifier system. Upon initialization, device calibration is performed to standardize sensor baselines. Continuous sampling of saliva enables electrochemical detection of pH and enzymatic detection of glucose or ions, while heart rate is acquired via PPG integrated near the pacifier's contact zone. The analog biosignals

Figure 3
Multifunctional smart pacifier system for continuous neonatal physiological monitoring

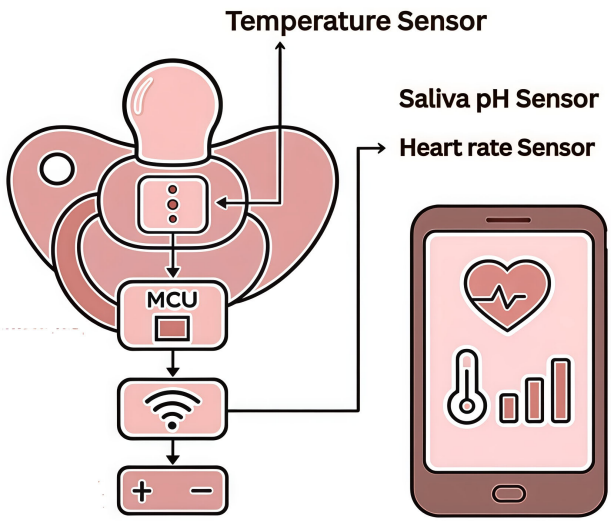

Figure 4
Smart pacifier operational workflow

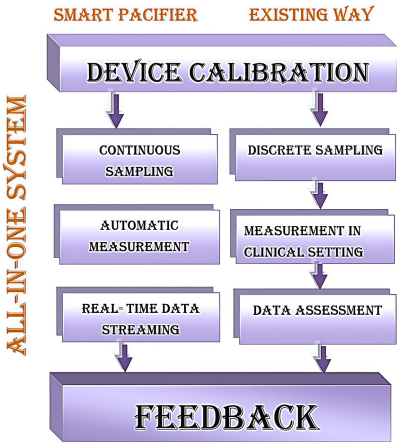

are routed through an analog front end (AFE), digitized by a low-power analog-to-digital converter (ADC), and processed by an onboard MCU utilizing embedded firmware for signal filtering and feature extraction. Wireless transmission modules (e.g., BLE) relay data to external interfaces for real-time visualization. Power management circuitry, including a micro battery and voltage regulators, supports uninterrupted operation, while the biocompatible enclosure ensures safe oral deployment over extended durations.

Although enzymatic amperometric and potentiometric biosensors embedded in flexible epidermal patches and smart pacifiers achieve exceptional sensitivity and precision—detecting salivary glucose with an LOD of ~0.7 nA/mM and demonstrating linearity of $R^2 \approx 0.994$—current validation cohorts predominantly include neonates with typical oral and craniofacial anatomy. Critically, infants presenting with anatomical or physiological anomalies, such as cleft palate (≈1:700 live births), tracheostomy (~0.1–0.3% of NICU admissions), or other congenital craniofacial malformations, remain largely unrepresented. Exclusion of these "long-tail" populations introduces a latent bias, potentially inflating reported device performance metrics and limiting translational applicability.

To address these gaps, future studies should adopt a stratified inclusion/exclusion framework. The core cohort should encompass full-term and preterm neonates without major anatomical abnormalities, establishing baseline sensor performance with quantified metrics such as signal-to-noise ratios (SNR > 20 dB), continuous monitoring fidelity (>95% valid sampling over 24 h), and calibration stability (<5% drift across 12 h). Edge-case cohorts, including infants with cleft palate, tracheostomy, or craniofacial anomalies, should undergo separate validation to quantify deviations in electrochemical and PPG signals. Preliminary modeling suggests that altered oral geometries could reduce enzymatic sensor contact efficiency by ~10–15% and attenuate PPG-derived heart rate signal amplitude by ~8–12%, underscoring the importance of dedicated evaluation. Transparent exclusion criteria should include conditions compromising safety, such as active oral infections or severe trauma, while ensuring data from medically complex neonates are captured whenever feasible. By harmonizing high-fidelity biosensing with inclusive cohort design, smart pacifiers can transcend conventional monitoring boundaries, delivering continuous, noninvasive insights across the full spectrum of neonatal physiology.

1) Spectroscopy-based wearables

Surface-enhanced Raman spectroscopy platforms, engineered as stretchable gold nanomesh films, offer label-free, on-skin molecular detection across a broad dynamic range (nanomolar to millimolar) [67]. These are capable of identifying sweat metabolites, exogenous drugs, and environmental toxins in real time. Nano-plasmonic optical sensors, such as functionalized Ag/Si nanowire arrays within smartwatch form factors, enable glucose monitoring via surface plasmon resonance shifts and Raman scattering, with demonstrated LODs as low as ≈ 0.12 mM [67].

3.1.3. Mechanical and motion monitoring

From postural analysis to muscular coordination, motion wearables have advanced from bulky pedometers to ultrathin, skin-like sensors capable of microsecond response times and nanometer precision. The section below recaps the leading categories within this domain.

1) Strain and pressure sensors (piezoresistive, capacitive, triboelectric)

Role: Transform mechanical deformation into electrical resistance or capacitance changes to detect body motion and tactile interaction. The following are the features:

a. Reduced graphene oxide–silver nanoparticle (rGO–AgNP) fabrics: These flexible, thermally resilient woven mats deliver ultrafast response times (<3 ms) and over 5,500 cycles of durability, enabling precise detection of gait phases, limb motion, and joint stress in dynamic activities. Studies report sensitivity ratios above 9.8 at 30% strain [68].
b. Triboelectric motion skins: Using nano-patterned Polyttetrafluoroethylene (PTFE) or Polyurethane (PU) surfaces, these systems generate electrical signals via body movement and environmental interaction, capable of self-powered tactile sensing in the micro-Newton range [69].

2) Textile-integrated and wearable fabric sensors

Role: Monitor respiration, posture, and muscular activity via fabric-based conductive sensors.

a. Conductive yarns made from PEDOT: PSS, silver-coated nylon, or screen-printed graphene are woven into garments to detect strain and pressure variations with minimal signal degradation during wear or wash [70].
b. Textile sensors are now being trialed in occupational safety (construction workers' fatigue tracking), maternal health (contraction monitoring), and child posture correction tools.

3) Pressure and muscle activity sensor arrays

Role: Map muscle contraction, limb pressure, and body loading for prosthetic support and movement reconstruction.

a. Sponge-based CNT/PDMS arrays: These devices offer localized pressure mapping using carbon nanotube-enhanced elastomers. A 16-channel flexible patch classified lower-limb motion with ≈97% accuracy, making it ideal for rehabilitation therapy, prosthetics, and stroke recovery [71].
b. Laser-patterned graphene electrodes: When combined with flexible gold circuits, these sensors achieve ultra-high strain resolution (≈0.024%) and exceptional gauge factors (GFs) ($\sim 6\times10^7$), supporting pulse tracking, hydration estimation, and breath monitoring in real time [72].

3.2. Organ-system–focused monitoring

1) **Skin and iontics:** Recent advances in epidermal sensing combine ECG with ionically conductive materials to achieve cuffless, continuous BP monitoring. A notable innovation is the dual-mode sensor integrating ECG electrodes with a pressure-sensitive ionogel substrate, which adheres comfortably to the wrist [73]. This patch simultaneously captures arterial pulse waveforms and ECG signals, enabling precise calculation of pulse transit time (PTT)—the delay between ECG R-wave and peripheral pulse arrival—correlated with systolic and diastolic BP values. Ionogels provide high ionic conductivity, mechanical flexibility, and skin conformability while maintaining signal stability under dynamic movements. Typical sensor thickness is under 100 microns, with sensitivity to pressure changes as low as 10 Pa, ensuring accurate PTT-based BP estimation without bulky cuffs [74]. Example: The Biobeat wearable wrist monitor uses PTT-based cuffless BP measurement combined with ECG, offering continuous BP tracking integrated with remote patient monitoring [75].
2) **Cardiovascular and in-sensor computing:** Ultra-flexible, stretchable organic electrochemical transistor (OECT) arrays represent a leap forward in on-skin biosignal processing. These arrays are fabricated via solution-processed printing of conjugated polymers onto elastomeric substrates, creating sensor matrices that directly transduce ionic currents from biofluids into electrical signals. OECTs inherently amplify weak biosignals such as ECG and EMG, allowing real-time edge computing at the sensor interface [76]. Their stretchability exceeds 30% strain without performance degradation, enabling seamless integration on curved skin surfaces. Operating voltages remain low (sub-1V), reducing power consumption significantly. Integration with flexible printed circuits enables in situ digital signal processing (DSP), noise filtering, and feature extraction, minimizing data transfer and preserving battery life in wearable platforms. Example: The IMEC's OECT patch prototype processes ECG and EMG signals locally, demonstrating on-skin computing capabilities that reduce latency and energy use, essential for next-generation wearable diagnostics [77].
3) **Musculoskeletal and motion:** Echomyography (EcMG) devices utilize a single wearable ultrasound transducer to noninvasively capture both muscle electrical activity and joint kinematics. This compact sensor emits pulsed ultrasound waves, reflecting from muscle tissues and joint interfaces to generate real-time imaging, while simultaneously recording mechanomyographic signals related to muscle contraction. The transducer typically operates at frequencies of 5–10 MHz with axial resolution below 0.5 mm, allowing detailed tracking of muscle thickness and joint angle changes during dynamic motion. Such integration aids rehabilitation by quantifying neuromuscular activation patterns and joint biomechanics without cumbersome multi-sensor setups [78]. Example: The Mysono EchoWear system is a wearable ultrasound platform developed for musculoskeletal assessment during rehabilitation, enabling portable and real-time joint and muscle monitoring [78].
4) **Brain and nervous system (cranial monitoring):** Noninvasive cranial monitoring employs discreet ear, EEG, and flexible headband electrodes to capture brainwave patterns, including delta (δ), theta (θ), alpha (α), beta (β), and gamma (γ) rhythms. Modern devices use dry-contact electrodes with impedances below 10 kΩ, enabling long-term wear without conductive gels. Super-thin e-tattoos, fabricated using photolithographically patterned carbon nanotube and graphene films, adhere to the forehead or postauricular skin with van der Waals forces [79]. These sensors, less than 500 nm thick, measure electrical potentials and eye movements (electrooculography [EOG]) with sampling rates exceeding 500 Hz and SNR above 20 dB. Data are transmitted wirelessly via BLE to smartphones or dedicated processing units. On the research front, organoid-on-chip platforms cultivate three-dimensional neural tissue mimicking human brain microenvironments within microfluidic chambers, enabling real-time electrophysiological recording and drug testing. Example: The Muse 2 EEG headband offers real-time brainwave monitoring for stress and sleep tracking, using dry sensors and wireless transmission to smartphones [80].

3.3. Wireless and self-powered systems

Wearable devices are increasingly engineered for autonomous operation, eliminating dependency on traditional batteries through energy harvesting and wireless power/data transfer. These systems integrate flexible harvesters, smart textiles, and wireless modules, enabling seamless power generation and real-time communication across dynamic environments.

1) Energy harvesting via mechanical, thermal, and bio sources: Piezoelectric and electromagnetic generators utilize human motion—such as joint bending—to generate electricity through cantilever-based structures, producing stable low-frequency outputs. Thermoelectric generators (TEGs) integrated into textiles—especially Mg-based materials—achieve ∼18.4 μW/cm² at 33°C under ∼0.8 kPa pressure. Advanced systems extract ∼91 μW from a 5°C gradient and operate at startup voltages as low as 62 mV. Bioenergy and sweat-evaporative harvesters leverage hybrid microgrids combining TEGs and biofuel cells to extract metabolic energy [81]. Notably, MXene–wool composite hydroelectric nanogenerators can power smartwatches via sweat evaporation [82].
2) Gel-based triboelectric nanogenerators (TENGs): Self-powered hydrogel-based TENGs convert mechanical inputs like motion or touch into electricity. These devices offer high flexibility and biocompatibility, enabling applications in wearable health monitoring and tactile interfaces, although long-term charge retention and durability require enhancement [83].

3) Self-healing, wireless, responsive materials: MXene-based ionotronic hydrogels exhibit dual energy harvesting via ultrasonic vibrations (up to 85 V) and RF stimuli (915 MHz), while also being self-healing. These materials wirelessly activate LEDs under ultrasound and support non-contact Radio Frequency Identification (RFID) sensing, presenting next-gen smart wearable capabilities [84].

4. Organ-Centric Wearable Diagnostics

Organ-centric wearable diagnostics encompass an advanced subset of bioelectronic systems that facilitate localized, continuous surveillance of specific organ-level physiological and pathophysiological parameters. These devices are anatomically optimized to conform to regions of clinical interest, such as thoracic ECG/PPG arrays for cardiac electrophysiology and hemodynamic profiling, periorbital graphene-based EOG interfaces for intraocular and oculomotor assessment, abdominal strain-gauge sensors for pulmonary kinematics, and epidermal microfluidic platforms for excreted metabolite quantification pertinent to hepatic or renal function. Neurological interfaces, including EEG-integrated headgear and in-ear electrophysiological monitors, further expand the domain to central nervous system diagnostics, enabling detection of cognitive states, sleep patterns, and early neural degeneration. Multimodal integration of electrophysiological (EEG, ECG, EMG), mechanoelectrical (strain, pressure), and electrochemical (sweat biomarker) sensing, when augmented with AI-driven signal processing and edge analytics, enhances spatiotemporal resolution, noise immunity, and clinical interpretability. These organ-specific platforms are pivotal for predictive diagnostics, chronic disease stratification, neurocardiovascular comorbidity mapping, and telemedical intervention, marking a transformative step toward precision digital medicine and bio-intelligent healthcare ecosystems.

4.1. Cardiovascular system

The advent of intelligent, ambulatory cardiovascular monitoring systems has enabled continuous electrocardiographic (ECG) surveillance via miniaturized, low-power, and biocompatible platforms. These systems incorporate biopotential electrodes, microcontroller-based acquisition circuits, textile-integrated sensors, and AI-enabled signal deconvolution algorithms, allowing high-fidelity cardiac diagnostics outside clinical environments. Comparative benchmarking of cardiovascular wearables requires alignment across AI models, subject demographics, hardware limits, and validation references. Table 3 condenses device-level metrics—spanning power budgets (<30 mW), inference latencies (<2 s), and clinical concordance (>85%)—to provide a reproducible baseline for translational and regulatory assessment.

4.1.1. Wireless ECG (biopotential wearables)

1) Bluetooth Low Energy (BLE) wrist-worn ECG modules: These modules operate as single-lead ECG acquisition systems embedded in ergonomically designed wristbands utilizing dry-contact Ag/AgCl electrodes positioned bilaterally [85].
   a. Functional architecture: The system comprises a differential AFE, coupled with a BLE SoC (e.g., Nordic nRF52840) that facilitates synchronized data acquisition between left and right wrists without reference electrode anchoring on the thorax [85].
   b. Electrophysiological fidelity: Demonstrated Pearson correlation coefficients ~0.84 with reference-standard Holter monitors for waveform similarity.
   c. Power profile: Sustains continuous operation for ~4.8 hours on 120 mAh lithium-polymer cells, with average system-level power consumption approximating 22–27 mW [85].
   d. Use case: Suited for longitudinal arrhythmia screening, stress diagnostics, and ambulatory rhythm monitoring in non-critical environments.

Figure 5 depicts the architecture of a BLE-enabled wrist-worn ECG biosensing module that integrates edge computing with real-time telemetry. The recording electrodes capture single-lead ECG signals, which are routed through a low-noise AFE with input-referred noise levels typically <1 μV RMS, ensuring signal fidelity for low-amplitude P-wave and ST-segment detection. The conditioned signals are digitized by a 12–16 bit ADC and processed locally on an ARM Cortex-M4 microcontroller (operating up to 80–100 MHz, ~5–10 mA active current). Complementary sensing modalities—SpO_2, accelerometry, and microphone inputs—support artifact rejection and multimodal health assessment. Data packets are transmitted via a 2.4 GHz BLE radio (e.g., Nordic nRF52840, BLE 5.0, throughput up to 2 Mbps) to external devices, enabling raw waveform streaming or parameterized data logging. A 120 mAh Li-polymer battery sustains ~4–5 hours of continuous ECG acquisition (system-level consumption 22–30 mW), with duty-cycled acquisition extending runtime to >24 hours. In validation studies, single-lead waveforms demonstrated Pearson correlation coefficients of 0.82–0.86 compared to Holter monitors, with HRV indices showing <5% deviation. The bi-directional Graphical User Interface (GUI) allows user control over recording parameters (channels, sampling rates of 250–500 Hz, bandpass filters 0.5–40 Hz) and provides clinicians with continuous, wireless access to electrophysiological data, supporting applications in arrhythmia screening, stress diagnostics, and ambulatory rhythm monitoring.

The selection of BLE for wrist-worn ECG modules is predicated on its optimal compromise between ultra-low latency, high-fidelity signal transmission, energy efficiency, and seamless user integration, parameters critical for continuous, clinical-grade biopotential monitoring. BLE enables short-range communication (≈5–10 m) with latency below 10 milliseconds, supporting uninterrupted streaming of multi-lead ECG signals to paired smartphones or proximal gateways while maintaining multi-day battery autonomy. In contrast, LoRaWAN affords long-range connectivity (up to several kilometers) but exhibits markedly limited throughput (0.3–50 kbps) and elevated end-to-end latency (hundreds of milliseconds), rendering it suboptimal for continuous ECG telemetry. NB-IoT presents intermediate coverage (1–10 km) with moderate data rates (20–250 kbps) and latencies between 100 and 500 ms. However, its comparatively higher energy expenditure and dependency on carrier-managed cellular infrastructure constrain its utility for compact, wearable ECG systems.

The trade-off matrix illustrated in Table 4 encapsulates performance as descripted below:

2) E-textile chest belts and smart garments: These wearable systems embed conductive polymer-based dry electrodes within textile substrates, interfaced with ferroelectric memory-based microcontrollers (e.g., TI MSP430FR series) for ultra-low power signal acquisition [86].
   a. Sensor mechanism: Textile electrodes with 3D looped microfiber geometries enhance conformal skin-electrode contact and minimize skin-electrode impedance (<10 kΩ) even during dynamic or aquatic motion.
   b. Signal processing: High-resolution ECG signals are digitized via 14-bit ADCs and transmitted via BLE 5.0 to paired mobile devices.

Table 3
Comparative matrix of algorithmic, hardware, and validation parameters for ECG-centric wearable systems

Device/Platform	Algorithmic Framework	Dataset Demographics and Size	Training and Hyperparameters	Hardware/Edge Constraints	Latency and Energy Benchmarks	Validation Baseline	Clinical Concordance
BLE Wristband ECG	Classical digital filtering + feature extraction; arrhythmia classification via logistic regression	120 volunteers (38 arrhythmic, 42 stress, 40 controls); age 22–70 yrs	Regularization $\lambda = 0.01$; 5-fold CV	Nordic nRF52840 SoC (64 MHz ARM Cortex-M4, 256 KB RAM); avg. power ~25 mW	Transmission + inference delay <200 ms	24-h Holter monitors	Waveform similarity $r \approx 0.84$
E-Textile Chest Belts	Support Vector Machine rhythm classifier	210 participants (55% male, 45% female), age 18–65; tested at rest and exercise	RBF kernel, $\gamma = 0.05$, $C = 1.0$; 10-fold CV	TI MSP430FR MCU (16 MHz, 128 KB FRAM); <500 µW consumption	Mean inference time ~0.6 s	Clinical 3-lead ECG	Accuracy 91.2%
mm-Wave Radar ECG	Deep CNN (7 conv layers, kernel 3×3, dropout 0.3); reconstructs PQRST morphology from displacement maps	1,400 recordings (650 healthy, 480 arrhythmic, 270 pediatric)	Adam optimizer, LR = 8e-4, batch = 64, epochs = 80	NVIDIA Jetson Nano (128 CUDA cores, 4 GB RAM); ~3.8 W	Sub-14 ms per cycle	3-lead ECG	Morphological fidelity ~90%; arrhythmia F1 ≈ 0.87
MXene Hydrogel ECG	Lightweight CNN denoiser + feature extractor (3 conv + 2 dense)	95 subjects; dynamic activity and cold-stress tests	LR = 1e-3, batch = 16, epochs = 50	STM32L4 MCU (80 MHz, 128 KB RAM)	Latency ~1.2 s; avg. 20 mW	Gel electrodes	+17 dB SNR improvement
FLEXER MXene Textiles	CNN-LSTM hybrid for ECG/EMG fusion and gesture recognition	72 participants under locomotion tasks	LR = 5e-4, batch = 32, epochs = 100	Nordic nRF52840 SoC; ~15 mW	~0.85 s latency	Commercial EMG armbands	Gesture detection accuracy ~93%
Graphene Tattoos (GETs 2.0)	Shallow CNN for multimodal fusion (ECG + arterial pressure + hydration)	50 participants; mixed activity states; 60% male, 40% female	LR = 1e-3, dropout = 0.25, epochs = 40	ARM Cortex-M33 MCU; ~18 mW	Inference cycle <1.5 s	Arterial tonometry + ECG	Pressure MAE ≈ 3.8 mmHg; ECG concordance ~87%

Figure 5
System architecture of a BLE-enabled wrist-worn ECG monitoring module

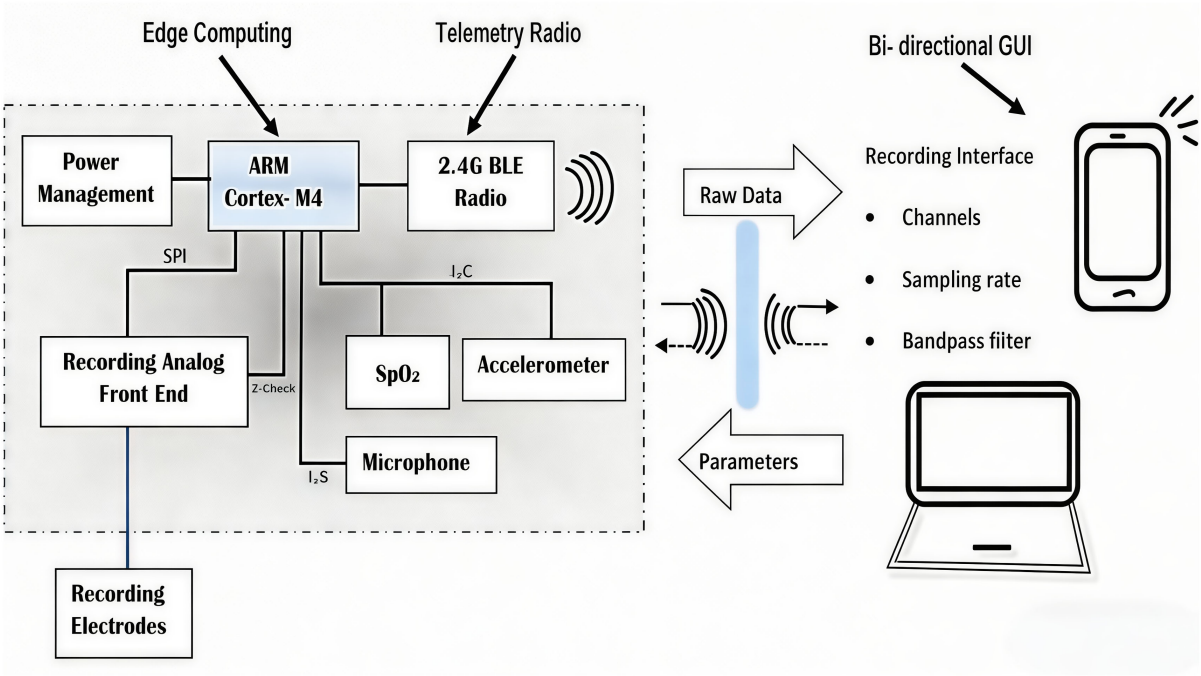

Table 4
Evaluation of latency, throughput, and energy efficiency in wireless technologies for ECG wearables

Wireless Technology	Effective Range	Latency	Data Throughput	Energy Profile	Suitability for Continuous ECG
BLE	5–10 m	<10 ms	Up to 2 Mbps	Ultra-low	Excellent
LoRaWAN	Several km	100–500 ms	0.3–50 kbps	Low	Poor
NB-IoT	1–10 km	100–500 ms	20–250 kbps	Moderate–High	Limited

c. Energy efficiency: Operates below 500 μW, ensuring extended battery longevity with coin-cell or flexible thin-film batteries.

3) Millimeter-wave radar–based contactless ECG: This novel modality employs Frequency-Modulated Continuous-Wave radar systems in the 60–77 GHz band to capture cardiogenic micromotions of the thoracic cavity, enabling non-contact ECG inference [87].

a. Mechanotransduction principle: Electromechanical transduction of ballistocardiographic and seismocardiographic signatures into ECG-equivalent waveforms using 4D radar imaging.
b. AI signal translation: Utilizes deep CNNs trained on synchronized ECG-radar datasets to reconstruct PQRST complexes from displacement signals.
c. Temporal resolution: Achieves sub-14 ms latency and waveform reconstruction with ~90% morphological fidelity to 3-lead ECG references.
d. Applications: Ideal for pediatric, geriatric, or infectious disease monitoring where skin-contact sensors are contraindicated.

4.1.2. MXene-based epidermal ECG platforms

Two-dimensional transition-metal carbides, notably $Ti_3C_2T_x$ MXenes, have emerged as exceptional materials for wearable ECG monitoring due to their superior electrical conductivity ($\sim 10^4$–10^5 S/m), hydrophilic surface terminations, and mechanical compliance. Their incorporation into hydrogel matrices and fabric systems has enabled skin-conformal, artifact-resistant, and high-resolution electrophysiological signal acquisition.

1) High-performance conductive hydrogel mechanics: MXene-infused hydrogels demonstrate enhanced mechanical integrity, freeze resistance (below −20°C), anti-dehydration barriers, and intrinsic self-healing over multiple damage cycles. These materials possess a GF ≥25, fast response times (~100 ms), and low impedance (<10 kΩ), ensuring accurate cardiac electrophysiological monitoring during dynamic activities [88].
2) Fabric-based lamina emergent MXene textile electrodes ("FLEXER"): Textile-integrated inflatable structures embedded with MXene-based electrodes provide adaptive, dry, contact ECG interfaces [89]. Upon pneumatic actuation, the system achieves laminar, skin conformation with low interfacial impedance (~5 kΩ), enabling artifact-free ECG/EMG monitoring under locomotion. Wireless data transmission modules allow integration with gesture recognition and remote monitoring platforms.

4.1.3. Graphene tattoo pressure sensors for cardiovascular monitoring

Graphene electronic tattoos (GETs) represent an ultrathin, conformal, and adhesive-free modality for continuous, noninvasive

arterial pressure and bioimpedance tracking at the wrist [90]. Leveraging the exceptional conductivity (~10^6 S/m), mechanical flexibility, and epidermal compatibility of monolayer graphene, these sensors are designed to seamlessly integrate with human biomechanics for high-fidelity cardiovascular diagnostics.

1) Next-generation GETs 2.0 enhancements: The GETs 2.0 platform introduces key nanostructural innovations that dramatically improve functionality and wearability [91]. Reinforced with multilayer graphene embedded with nanoscrolls and engineered micro-perforations, these updated tattoos offer enhanced electrical stability and sweat permeability while maintaining a sub-500 nm ultralight thickness. These modifications result in a ~3.5× reduction in sheet resistance and ~2.5× decrease in skin–tattoo impedance, facilitating uninterrupted biopotential acquisition over extended durations. The perforated architecture achieves a sweat permeability rate of ~3200 g m² day, ensuring signal integrity and user comfort. GETs 2.0 also exhibit multimodal capabilities, simultaneously capturing ECG signals, hydration levels, and other vital signs in addition to arterial pressure.
2) Biomechanical conformity and sensor-skin integration: Engineered to match the skin's low Young's modulus (~70–100 kPa) and maintain a sub-100 μm mechanical profile, graphene tattoos achieve exceptional conformal adhesion with minimal interference to natural epidermal motion [92]. This close lamination significantly reduces motion-induced artifacts during wrist flexion or hand gestures, preserving stable impedance readings even under sweat or mechanical stress. The device's bioinspired mechanical design facilitates near-invisible integration, offering long-term user compliance, high signal fidelity, and robust compatibility with daily physiological activities.

4.2. Respiratory system

1) Lung–Sound–Monitoring–Patch (LSMP): The LSMP is a skin-adhered, biocompatible auscultation device engineered for continuous cardiopulmonary sound acquisition [93]. The core sensing system integrates uni- and omnidirectional MEMS microphones encased within a custom 3D-printed resin housing, ensuring structural integrity and biocompatibility. Its acoustic conduit design filters ambient environmental noise and amplifies thoracic acoustic transduction for improved SNR. An MCU processes real-time data on board, while power is sustained via a LiPo (Lithium Polymer) battery, all compactly embedded without mechanical protrusion. The assembly is affixed to the thoracic region using medical-grade adhesive to maintain tight skin contact during locomotion, minimizing mechanical artifacts. LSMP's acoustic signals undergo real-time denoising and classification via an onboard AI system trained on a 2D CNN architecture. The neural engine processes audio inputs across time-frequency spectrograms, effectively distinguishing respiratory events such as wheezes and crackles. Clinical trials demonstrated ~80.5% concordance with pulmonologists' assessments in COPD and pediatric asthma patients.
2) Graphene oxide (GO) triboelectric respiratory sensor: The core transduction mechanism of the GO triboelectric respiratory sensor is built upon triboelectric nanogenerator (TENG) principles [94]. GO—rich in oxygen-containing functional groups and possessing a high surface area layered structure—acts as an optimal triboelectric layer. In wearable constructs, GO is typically embedded into hydrogel matrices (e.g., chitosan, GO composites) or coated onto flexible substrates like elastomeric films or textile masks. Upon inhalation and exhalation, the resulting mechanical deformation drives contact-separation cycles between the GO layer and a counter-electrode material. This dynamic interface modulates triboelectric charge generation, resulting in measurable AC voltage pulses corresponding to the respiratory flow and humidity shifts. GO-based TENG respiratory sensors exhibit rapid temporal resolution (<100 ms), enabling precise tracking of respiratory rate and depth. Their high tribosensitivity allows for the detection of even microscale airflow and humidity fluctuations linked with shallow breathing or early pathological symptoms. Mechanically, the sensor maintains ultra-lightweight, thin-film flexibility, allowing conformal integration onto facial masks, thoracic patches, or wearable fabrics. The self-powered GO-TENG architecture converts respiratory airflow into electrical signals, eliminating the need for external batteries [95]. This enables long-term, maintenance-free monitoring, ideal for conditions like sleep apnea and COPD. Integration with low-power wireless modules (e.g., Bluetooth, NFC) supports real-time, remote data transmission without additional energy input.

Table 5 summarizes edge AI respiratory wearables that implement CNN or CNN-LSTM models on ARM Cortex-M4/M7 or Nordic nRF52840 MCUs, achieving <2 s inference and <30 mW power draw. Training datasets span 2,500–3,500 multi-site recordings (pediatric to elderly, balanced gender), with outputs validated against spirometry, capnography, or pulmonologist consensus, enabling standardized benchmarking of accuracy, latency, and physiological fidelity.

4.3. Nervous system

1) **Graphene electronic skin for EMG/EOG monitoring:** Graphene-based electronic skins (e-skins) provide an ultrathin, breathable, and imperceptible platform for high-fidelity recording of EMG and EOG signals. The innovations in graphene e-skin biointerfaces are listed below:
   a. Graphene EOG tattoos: Imperceptible graphene e-tattoos (GETs), laminated around the eye without adhesives, enable angular eye tracking (~4° resolution) and real-time device control, such as operating quadcopters via wireless EOG signals [96].
   b. High-performance EMG graphene skins: Laser-scribed graphene e-skins, directly transferred onto the skin, function as substrate-free conductors [97]. They drastically reduce skin-electrode impedance, enhancing signal amplitude and SNR. These e-skins remain functional under >60% strain and 1,000+ stretch cycles, enabling stable EMG monitoring during motion.
2) **Neural-signal and biochemical sensing headbands:** Recent innovations in wearable neurotechnology have led to multifunctional headbands that integrate neural signal acquisition with physiological and biochemical sensing, enabling real-time brain–computer interfacing and holistic health monitoring. The following are the advances:
   a. Cognionics Quick-20 and AI-powered EEG interpretation: The Cognionics Quick-20 headband uses four dry electrodes, following the 10-20 system, to record EEG signals without the need for conductive gels [98]. When

Table 5
Edge, deployed AI architectures and clinical baselines for next, generation respiratory wearable

Device	Algorithmic Framework	Dataset Composition	Training/ Hyperparameters	Edge Deployment Constraints	Latency and Power Benchmarks	Validation Baseline	Clinical Performance
Lung–Sound– Monitoring– Patch (LSMP)	2D CNN (spectrogram-based), 5 conv layers, ReLU activation, max-pooling; softmax classifier	2,600 lung sound recordings (COPD = 780; pediatric asthma = 520; healthy = 1,300); ages 5–72 yrs; 42% female; collected across 3 clinical sites	LR = 0.001; batch size = 32; epochs = 60; dropout = 0.4	ARM Cortex-M7 MCU (600 MHz, 1 MB SRAM, onboard DSP); optimized with quantization-aware training	End-to-end inference <1.9 s; avg. compute load 30 MFLOPs; sustained power draw 28 mW	Compared with pulmonologist consensus and Littmann 3200 digital stethoscope outputs	AI concordance 80.5% vs. pulmonologists; +12% accuracy gain over FFT + threshold baseline
GO-TENG Respiratory Sensor	Hybrid CNN-LSTM (3 conv layers + 1 LSTM, 128 hidden units) for temporal airflow mapping	3,400 respiration cycles (healthy adults = 60; COPD = 25; sleep apnea = 18); balanced gender; multi-site	LR = 0.0005; batch size = 64; epochs = 100; early stopping	Nordic nRF52840 SoC (ARM Cortex-M4, 64 MHz, 256 KB RAM); model compression via pruning	Inference latency ~850 ms per cycle; compute load 45 MFLOPs; avg. power <12 mW (self-powered via TENG)	Benchmarked against spirometry and capnography outputs	Respiratory rate detection accuracy 94.1%; micro-breath sensitivity +17% vs. peak-threshold baseline

paired with AI models like 1D-CNN and LSTM networks, it can identify motor imagery, such as left or right hand movement intent, in under 2 s and reach up to 92% accuracy. Still, there is a key limitation: long-term validation for changes in AI model performance over time is lacking. For example, a pilot study using edge-based CNN/LSTM classifiers in outpatient neurorehabilitation found that accuracy dropped from 90% at the start to about 74% after 15 months of ongoing use. This decline was linked to changes in scalp-electrode impedance, individual neuroplasticity, and more noise in everyday settings. These findings highlight the need for regular recalibration and adaptive updates, including methods like transfer learning and federated model optimization.

b. Muse S and BrainsBit for multimodal biofeedback: Consumer neurobands like Muse S and BrainsBit integrate 4-channel EEG sensors with additional PPG modules for real-time heart rate and respiration tracking [99]. Higher-end models offer optional functional near-infrared spectroscopy (fNIRS) to monitor cerebral oxygenation. These devices translate mental states into audio-visual feedback for meditation, stress reduction, and sleep optimization.

c. NeuroLife headband with metabolic integration (prototype stage): Experimental platforms such as the NeuroLife Biochem Band are exploring the integration of electrochemical biosensors into EEG headsets [100]. Sweat-analyzing modules for glucose and lactate enable dual-mode monitoring of cognitive and metabolic stress. These prototypes hold promise for next-generation neurochemical diagnostics in stress physiology and cognitive workload assessments.

3) **Wearable EEG/EOG dry electrode systems:** Dry-contact electrode technologies are revolutionizing neural and ocular biosignal acquisition by enabling long-duration, gel-free EEG and EOG monitoring with enhanced comfort, mobility, and clinical-grade fidelity. Below are the views on advancements:

a. Conductive polymer dry electrodes (PEDOT: PSS-based system): Next-generation dry electrodes composed of a PEDOT: PSS–polyurethane–D-sorbitol composite exhibit excellent skin adherence, stretchability, and conductivity [101]. These organic polymer-based patches deliver stable EEG, ECG, and EMG signals across variable conditions and outperform Ag/AgCl gel electrodes in motion-prone scenarios—ideal for real-time arrhythmia and muscle activity monitoring.

b. Ultrathin epidermal electrodes (<100 nm): Conformal nanosheet electrodes (~100 nm) designed to match skin topography offer nearly invisible and adhesive-free integration [102]. Their ultra-low impedance and motion artifact resistance enable high-fidelity EEG recording with minimal baseline drift during facial movement or exertion.

c. Active spring-loaded electrode arrays: Mechanically adaptive spring-loaded dry electrode arrays incorporate buffer amplifiers within each "finger-like" probe [103]. These active sensors achieve <1.13 μV RMS noise and superior alpha-wave capture by maintaining stable scalp contact—even through hair—while compensating for mechanical shifts.

d. GAPses smart glasses for EEG/EOG: GAPses is an experimental smart-glasses prototype embedding dry EEG/EOG electrodes within the frame [104]. With edge AI processors and ultra-low power consumption (~16 mW), it enables 12-hour continuous use and achieves 98–99%

classification accuracy of cognitive and ocular states, suitable for BCI and behavioral analytics.

4) **Driver drowsiness detection eyewear:** Wearable smart glasses and headgear are emerging as efficient solutions for real-time drowsiness monitoring, leveraging dry electrodes, ocular tracking, and AI-driven signal processing to detect fatigue-related neural and visual biomarkers with minimal user intrusion. Below are the views on advancements:

   a. Camera-embedded smart glasses with EOG analytics: A prototype optical-path smart eyewear system incorporates a miniaturized temple-mounted camera and hot-mirror optics to noninvasively capture eye movements [105]. A lightweight CNN processes visual cues such as blink rate and PERCLOS (Percentage of Eyelid Closure) with accuracy rivaling clinical EyeLink platforms, enabling precise fatigue detection in mobile settings.
   b. In-ear EEG for neural fatigue monitoring: Dry electrode EEG earbuds, embedded within the auditory canal, detect changes in alpha and theta brainwave activity indicative of early-onset drowsiness [106]. These compact, gel-free biosensors support continuous, discreet monitoring during driving and have potential for integration into advanced driver-assistance systems.

Table 6 presents neural and ocular wearables with end-to-end AI pipelines, including CNN, LSTM, and hybrid architectures. Training cohorts range from 10 to 110 healthy participants, covering cognitive, motor, and ocular tasks. Edge deployment is achieved on low-power MCUs (16 mW–5 W) and embedded processors, ensuring sub-2 s inference latency. Validation is performed against clinical EEG/EOG systems or behavioral benchmarks, allowing comparative assessment of signal fidelity, classification accuracy, and real-time feasibility.

The validation cohorts employed in contemporary neural and ocular wearable studies, as delineated in Table 6, are predominantly restricted to ostensibly healthy, demographically homogeneous populations, including university affiliates, office-based professionals, and short-term trial participants. While such cohorts facilitate controlled benchmarking of device algorithms against gold-standard EEG and electrooculographic (EOG) recordings, they inadequately encapsulate the phenotypic and physiological heterogeneity inherent in real-world populations. This limitation may obscure critical inter-individual variability in neurophysiological dynamics, ocular function, cognitive load, and device usability across diverse demographic and occupational strata.

1) **Socioeconomic status (SES) and device engagement:** SES significantly influences both health outcomes and technology engagement. For instance, higher SES is generally associated with better ocular health and greater adherence to device protocols, whereas lower SES populations may face barriers to accessibility and sustained use. A cohort study involving 10,414 children revealed that Black children and those from lower SES households were less likely to enroll and wear devices for significantly less time compared to their White and higher SES counterparts. This disparity highlights the need for inclusive recruitment strategies that consider SES to ensure equitable data collection.
2) **Educational background and health literacy:** Educational attainment affects health literacy, which can shape an individual's ability to interpret wearable outputs. Participants from lower educational backgrounds often demonstrate shorter engagement and reduced compliance, indicating that validation studies should account for educational diversity to improve usability and adherence.
3) **Occupational exposure and physiological variations:** Occupational factors can uniquely influence neural and ocular physiology. For instance, individuals in mining environments may experience particulate and noise exposure, while those in IT sectors may face prolonged screen exposure. These occupational exposures can affect device performance, such as signal fidelity and classification accuracy. However, such occupational cohorts remain largely absent from existing studies, suggesting a gap in current validation practices.
4) **Age and ocular biometrics:** Age-related physiological changes can impact the performance of ocular biometrics. A study evaluating ocular biometrics across different age groups found equivalent performance in user verification and gender classification among young, middle-aged, and older adults. However, performance differences were noted at lower false match rates for older adults and at age classification for younger adults, suggesting that age diversity is crucial in validation studies to ensure fairness and accuracy.
5) **Racial and ethnic diversity in wearable studies:** Racial and ethnic diversity is essential for the generalizability of wearable technologies. Studies have shown that Black and Hispanic children are less likely to participate in wearable device studies and exhibit shorter device wear times compared to their White counterparts. This underrepresentation can lead to biases in data collection and device performance, underscoring the need for diverse validation cohorts.

5. Multimodal and Hybrid Wearable Platforms

Multimodal and hybrid wearable platforms embody the convergence of electrophysiological, biochemical, and mechanical sensing within ultrathin, stretchable electronics, enabling continuous, noninvasive health monitoring with clinical-grade precision. Developed through foundational work by Prof. John A. Rogers (epidermal electronics), Prof. Zhenan Bao (conductive polymers and nanocomposites), and Prof. Takao Someya (organic electronics), these devices integrate sensor arrays—including electrocardiographic (ECG, 250–500 Hz, SNR ∼30–40 dB), photoplethysmographic (PPG), amperometric glucose sensors (LoD ∼1–5 μM), ion-selective potentiometric sweat sensors (selectivity coefficients down to 10^{-3}), thermistors (resolution ±0.01°C), and inertial MEMS (accelerometers, gyroscopes)—onto biocompatible substrates such as polyimide (PI), polydimethylsiloxane (PDMS), or Ecoflex with stretchability >30% and conformability <10 kPa modulus [107]. Hybrid integration strategies use serpentine interconnects, island-bridge configurations, and 3D multilayer stacking to optimize spatial density and mechanical resilience. AI modules developed by Prof. Dina Katabi (MIT) and signal-fusion frameworks by Dr. Ali Javey (UC Berkeley) enable real-time classification and predictive analytics via CNNs and CNN pattern recognition with latency <100 ms [108]. Wireless transmission is achieved through BLE 5.0 (range: ∼10–30 m), NFC, or LoRa, supported by energy-harvesting units, including flexible photovoltaics (power density of up to 20 μW/cm² under ambient light) and biofuel cells. Clinically validated devices have demonstrated efficacy in neonatal care (e.g., wireless ECG patches reducing electrode-induced skin trauma), heart failure detection (e.g., thoracic impedance trends pre-empting decompensation), and diabetes monitoring (e.g., sweat lactate correlating with blood glucose, R^2 ∼0.91).

Table 6
AI specifications and validation outcomes for neural and ocular wearable devices

Device/Platform	AI/ML Framework	Dataset Demographics	Training Details and Hyperparameters	Hardware and Compute Constraints	Latency/Runtime	Validation Baseline	Reported Performance
Graphene EOG Tattoos (GETs)	CNN classifier for angular eye tracking (using bidirectional GUI)	18 healthy volunteers; indoor navigation tasks	3-layer CNN, kernel 3×3, dropout = 0.25, LR = 1e-3	ARM Cortex-M4F MCU; ~22 mW power budget	<250 ms inference	Clinical EOG electrodes	Angular resolution ~4°, quadcopter control success ~93%
High-Performance EMG Graphene Skins	Random forest classifier (gesture decoding)	25 healthy subjects; 1,000+ stretch-motion recordings	200 trees, depth = 15, 10-fold CV	STM32L4 MCU, 80 MHz	~0.9 s	Gel-based Ag/AgCl EMG	Gesture recognition accuracy ~90%
Cognionics Quick,20	Hybrid 1D-CNN + LSTM for motor imagery	32 subjects, 60% male, 40% female; no pathology inclusion	CNN: 64 filters, kernel 5; LSTM hidden size 128; epochs = 80	Intel i7 laptop + optional Jetson Xavier NX	1.8–2.0 s	32-channel gel EEG (BioSemi)	Motor intent accuracy ~92%
Muse S/BrainsBit Neurobands	CNN + unsupervised clustering for biofeedback states	110 users across meditation/sleep trials	CNN with 5 conv layers, batch = 64, LR = 8e-4	BLE 5.0 MCU + smartphone	~0.6–0.8 s	Polysomnography (EEG + PPG)	Sleep stage concordance ~82%
NeuroLife Biochem Headband (Prototype)	Multimodal CNN fusing EEG + sweat biosignals	Pilot n = 10; healthy male adults, exercise-induced stress	Early fusion CNN, 4 conv layers + dense; Adam, LR = 1e-3	Raspberry Pi CM4; ~5 W	~2.2 s	Lab-based lactate assays	EEG + metabolic dual-signal feasibility; no clinical-grade validation
PEDOT:PSS Dry Electrode EEG	CNN-LSTM hybrid for EEG/EMG	45 volunteers (dynamic + rest states)	CNN (3 conv), LSTM hidden = 64, dropout = 0.2	TI MSP430 MCU; <500 µW	~1.1 s	Gel Ag/AgCl electrodes	SNR gain +12 dB vs. gel
Ultrathin Epidermal Nanosheet Electrodes	Denoising autoencoder (EEG artifact reduction)	22 subjects; exercise + facial expression stress tests	Autoencoder latent dim = 128, epochs = 50	Cortex-M33 MCU; 16 mW	~1.5 s	EEG cap (32 ch)	Artifact suppression ~88%
Active Spring-Loaded Arrays	CNN with attention for alpha-wave capture	20 subjects; resting state + eyes-closed trials	5 conv layers, attention head dim = 64	Jetson Nano; ~4 W	<300 ms	Ag/AgCl EEG	RMS noise ~1.13 µV; Alpha detection precision ~95%
GAPses Smart Glasses	Edge CNN (6 conv layers) for EEG/EOG fusion	34 participants; mixed cognitive tasks, ~12 h sessions	LR = 5e-4, dropout = 0.3, epochs = 100	Ultra-low power MCU (~16 mW)	Real-time	EyeLink 1000, 32-ch EEG	Cognitive/ocular classification

5.1. Soft microfluidic and electrochemical hybrid patches

Soft microfluidic–electrochemical hybrid platforms integrate elastomer-based microchannel networks with potentiometric and amperometric biosensors for noninvasive, real-time sweat diagnostics. These epidermal devices utilize capillary-driven microfluidics with hydrophilic–hydrophobic patterning to route sweat to screen-printed electrodes (e.g., Ag/AgCl, carbon, Prussian blue [PB]) on substrates such as PDMS or Ecoflex [109]. Biomarker panels—including sodium (Na^+), potassium (K^+), lactate, uric acid, pH, and cortisol—are quantitatively analyzed via ion-selective electrodes and enzymatic reaction-based electrochemical transduction. Embedded low-power electronics and BLE modules facilitate wireless telemetry and integration with mobile interfaces. Compared to uniparametric consumer-grade wearables, these multiplexed systems enable molecular-level surveillance relevant to conditions such as hypertension, gout, electrolyte imbalance, and diabetes. Critical limitations include analyte dilution, inter-/intra-individual variability in sweat composition, calibration instability, and low SNR at micromolar detection thresholds. Advancements in nanostructured electrode materials, self-powered electronics (e.g., TEGs, Organic Photovoltaic (OPVs)), and AI-based signal deconvolution are accelerating their evolution toward robust, predictive, and scalable chronic disease monitoring platforms. Emerging wearable innovations in sweat-based biochemical and cardiovascular monitoring are explained below:

1) **Microfluidic-integrated glucose-ECG patch (thin and flexible):** In July 2023, a multidisciplinary research team reported the development of a fully integrated, epidermal biosensing platform that enables simultaneous real-time monitoring of sweat glucose concentration and electrocardiographic (ECG) activity within a single soft, stretchable microfluidic patch [110]. The device comprises a microfluidic-enabled PDMS substrate incorporating capillary microchannels that direct eccrine sweat toward a reduced graphene oxide (rGO)-based enzymatic glucose sensor. The sensor operates via glucose oxidase (GOx)-mediated catalysis and PB electrocatalysts, achieving a sensitivity of approximately 19.97 $\mu A \cdot mM^{1} \cdot cm^2$ and a linear detection range from 10 µM to 0.4 mM. The microfluidic design significantly enhances analyte delivery efficiency and minimizes cross-contamination, enabling stable, low-noise current responses under dynamic physiological conditions. In parallel, biopotential monitoring is facilitated by laser-patterned MXene–poly(vinylidene fluoride) carbon nanofiber electrodes functioning as dry ECG interfaces, exhibiting low skin–electrode impedance (~40.5 $k\Omega \cdot cm^2$) and a high SNR (23–33 dB), comparable to Ag/AgCl gel-based electrodes [110]. Integrated temperature and pH sensors provide dynamic compensation to correct enzymatic and electrochemical response drift associated with sweat composition and environmental changes. A flexible printed circuit board (FPCB) embedded within the patch hosts AFE circuitry, ADCs, memory units, voltage regulators, and a BLE transceiver to enable continuous, wireless telemetry. Real-time signal acquisition and synchronization are achieved through onboard data processing algorithms and multiplexed sensor interfaces. The platform underwent on-body validation involving five human subjects exposed to thermally induced perspiration (sauna environment) and moderate physical exercise, confirming operational stability under biomechanical strain and variable sweat generation rates. The patch maintained consistent glucose readings and high-fidelity ECG signal acquisition over multiple trials, highlighting its robustness and translational potential. This system represents the first reported example of a stretchable, soft-material-based epidermal patch integrating enzymatic glucose sensing and high-fidelity ECG recording into a single autonomous platform. Its modular, miniaturized architecture and high analytical precision underscore its potential as a next-generation diagnostic tool for noninvasive, multimodal, real-time monitoring in metabolic and cardiovascular disease management.
2) **Sweat rate and ion panel patch:** This epidermal wearable biosensing system integrates a flexible spiral microfluidic channel with multiplexed ion-selective electrochemical sensors and impedance-based sweat rate sensing, forming a comprehensive, skin-interfaced hydration monitoring platform. The microchannel, laser-micropatterned into PET/PDMS layers (~100 µm height, 1 mm width, ≈350 mm total length), facilitates capillary-driven, directional sweat transport while minimizing dead volume, air entrapment, and evaporative losses [111]. Embedded interdigitated gold electrodes within the microchannel act as impedance transducers, detecting volumetric sweat accumulation in real time. Adjacent to this region, ion-selective electrodes functionalized with membrane chemistries enable potentiometric quantification of key analytes—sodium (Na^+), potassium (K^+), chloride (Cl^-), and hydrogen ions (pH)—as the sweat traverses the channel. The integrated FPCB performs on-patch signal conditioning via ADCs, microcontroller-based drift correction algorithms, and wireless telemetry (e.g., via Bluetooth). Validated in both controlled laboratory settings and field trials, the platform demonstrates sweat flow rate accuracy within ±10% compared to commercial sensors and stable ionic detection across varied perspiration conditions (0.2–4 µL/min flow range). Its microfluidic design prevents sweat mixing or stagnation, ensuring continuous, time-resolved biomarker profiles. This multimodal device holds clinical and field utility for dehydration assessment, electrolyte imbalance monitoring, exertional heat stress, and salt-losing pathologies, with real-time analytics empowering both individual users and clinicians. Figure 5 presents the system-level architecture of a sweat biosensing platform. Sweat is first extracted and guided through microfluidic channels (typical dimensions: ~80–120 µm height, 0.8–1.2 mm width) to the electrochemical transducer for analyte detection. The AFE conditions signals within the range of 1–100 mV, followed by amplification (up to 10^3 gain) and conversion through a 12–16 bit ADC/DAC, ensuring sensitivity to ionic fluctuations as low as 1 mM. A low-power microcontroller (e.g., ARM Cortex-M0/M4 class, <10 mW consumption) executes digital filtering, drift correction, and temporary memory storage (≈256 kB–1 MB). Wireless telemetry is achieved via BLE (data rates up to 1 Mbps, range ~10 m) or NFC modules, enabling seamless communication with external devices. The power management circuit regulates operation from a thin-film battery (1–3 V, 10–20 mAh capacity), providing continuous monitoring for 12–24 hours. This configuration has been validated to capture sweat flow rates in the 0.1–5 µL/min range with volumetric accuracy within ±8–10% and to support stable potentiometric measurements of Na^+, K^+, Cl^-, and pH across varying perspiration conditions.
3) **Low-cost printed microfluidic patch for cortisol and glucose:** This ultrathin, epidermal "smart bandage" integrates inkjet-printed electrochemical biosensors and laser-patterned

microfluidic channels onto a flexible PI substrate, enabling real-time, noninvasive monitoring of glucose and cortisol levels in human sweat [112]. The device, approximately 78 mm × 20 mm in dimension, employs high-resolution (1270 dpi) printed graphene and Ag/AgCl electrodes thermally cured at 350°C for structural stability. A PET top layer with a hydrophilic surface ensures capillary-driven sweat transport along a 1 mm-wide microchannel, terminating in an absorbent pad that maintains continuous flow via passive evaporation. Adhesive microstructures define channel geometry and enable skin adhesion without compromising permeability or flexibility. The glucose sensing module consists of a two-electrode configuration—graphene working and Ag/AgCl counter/reference—functionalized with glucose oxidase (GOx). Enzymatic oxidation of glucose to hydrogen peroxide is electrochemically transduced at ∼0 V, offering a physiologically relevant dynamic range (0.2–1.0 mM) with a detection limit of ∼10 μM at sweat flow rates ≥2 μL/min. For cortisol detection, a three-electrode chronoamperometric architecture is employed. The graphene/AuNP working electrode, modified with immobilized anti-cortisol antibodies, enables highly specific immuno-detection of cortisol via redox signal modulation, achieving a limit of detection down to 10 pM. A climactic innovation is the incorporation of an electrowetting valve (fabricated using Perfluorodecanethiol (PFDT)-modified silver ink) that provides electrically tunable flow control, mitigating premature mixing and enhancing temporal resolution of biomarker sampling [112]. The patch demonstrates exceptional mechanical resilience, retaining sensor functionality under bending, twisting, and dynamic strain, making it suitable for use on curved anatomical regions such as joints. Although the current iteration does not detail onboard electronics, the system is compatible with external or integrated data acquisition modules for signal digitization and wireless transmission to mobile interfaces. This dual-analyte sweat biosensor represents a significant advance in wearable diagnostics by enabling continuous cortisol–glucose tracking with picomolar to micromolar sensitivity under physiological flow conditions.

5.2. Wireless integrated sensor systems (WISS)

A 3D-printed epidermal patch integrates microfluidic channels and bio-functionalized electrochemical electrodes for multiplexed sweat biomarker detection—specifically glucose, lactate, and uric acid. Designed for on-body applications under dynamic physiological conditions, this platform enables real-time, on-demand biochemical readout without external instrumentation. Each biosensor utilizes distinct enzymatic redox reactions resulting in visible colorimetric transitions, with hues corresponding to target analyte concentrations—red for glucose, green for lactate, and blue for uric acid. The microfluidic architecture ensures directional sweat transport via passive capillary action, preventing analyte cross-contamination. Fabricated via single-step additive manufacturing, this low-cost, flexible device demonstrates high mechanical compliance, stability during motion, and direct visual readout, validated under exercise-induced perspiration. This prototype exemplifies the convergence of colorimetric biosensing, microfluidics, and accessible fabrication toward self-contained, personalized health monitoring platforms.

1) Design architecture and biochemical specifications:

a. Substrate and structure: Flexible, biocompatible polymer substrate with embedded microchannels and biosensors, printed via additive manufacturing in a monolithic process.
b. Analytes detected: Glucose, lactate, uric acid.
c. Sensing mechanism: Each analyte-specific electrode is coated with a dedicated enzymatic reagent that catalyzes a redox reaction upon contact with the target molecule. The product of this reaction induces a colorimetric shift proportional to concentration.
d. Microfluidic channeling: Capillary-driven passive fluidic system directs sweat toward isolated detection chambers, ensuring laminar flow and preventing analyte cross-interface.
e. Colorimetric electrodes: Chemically functionalized sensors that operate via visible chromogenic transformation, enabling direct optical readout without the need for electronic circuitry.
f. On-body validation: Demonstrated effective performance under physical exertion—conforming to the skin, maintaining contact, and yielding biochemical feedback during sweating and movement.

2) Mechanism of operation:

a. Sweat collection via capillary action: As eccrine sweat glands secrete fluid, it is passively wicked into the hydrophilic microfluidic channels, guided toward the biosensor chambers through surface tension and microchannel geometry.
b. Analyte-specific enzymatic reaction: Upon contact with the bioelectrode surface:
c. Glucose reacts with glucose oxidase (GOx)
d. Lactate reacts with lactate oxidase (LOx)
e. Uric acid undergoes enzymatic oxidation via uricase

These reactions generate intermediate species (e.g., H_2O_2), which trigger a colorimetric reaction (likely mediated by peroxidase-mimicking chromophores).

3) Color change for visual quantification:

The chromogenic response produces a concentration-dependent hue visible to the naked eye. The sensor regions exhibit: red for glucose accumulation, green for elevated lactate, and blue for high uric acid levels.

4) Immediate visual feedback:

The patch is fully passive, requiring no power, display, or interface. Users observe color intensity directly to gauge relative biochemical levels.

5) Mechanical robustness and wearability:

Due to its thin and flexible architecture, the patch adheres seamlessly to skin contours, maintains structural integrity during bending, and preserves signal fidelity during physical motion.

5.3. BLE and NFC-based wireless interfaces

NFC and BLE are foundational short-range wireless protocols integrated into wireless integrated sensor systems for healthcare applications [113]. Operating at 13.56 MHz, NFC enables secure, low-latency (<0.1 s), and proximity-bound (≤4 cm) data exchange through inductive coupling. Its passive architecture leverages electromagnetic field harvesting, allowing battery-free operation in smart tags, access modules, and point-of-care data transfer. Conversely, BLE functions over the 2.4 GHz ISM band with adaptive frequency hopping and ultra-low power consumption (∼0.01–0.5 W), supporting extended-range (up to 100 m) and continuous telemetry [114]. Modern BLE 5.2 modules enable bidirectional communication, audio streaming, and mesh networking, rendering them suitable for persistent biosignal transmission from wearable biosensors.

1) Mechanistic Integration in IoMT:

a. Enabling secure patient authentication by inductively coupling NFC-tagged epidermal patches with clinical readers, exploiting 13.56 MHz passive communication for identity verification.
b. Activating real-time localization of patients, clinicians, and medical assets via BLE beacon triangulation, employing Received Signal Strength Indicator (RSSI)-based signal strength analysis and adaptive frequency hopping across the 2.4 GHz ISM band [115].
c. Implementing dual-mode telemetry by integrating hybrid NFC-BLE transceivers, enabling passive analyte sensing (e.g., glucose oxidase-based fingertip wrap) and continuous biosignal streaming (e.g., HRV, ECG) through BLE modules.

6. Clinical Translation and Regulatory Landscape

1) Challenges in clinical validation

Clinical validation is a post-claim forensic process in which licensed clinicians verify that diagnoses and procedure codes—such as ICD-10-CM and CPT—are supported by clinical evidence, including lab results, imaging, treatments, and progress notes. This process is mandated under Health Insurance Portability and Accountability Act (HIPAA) (1996) in the United States, enforced through the False Claims Act (31 U.S.C. §§ 3729–3733), and further reinforced via Section 6401(a) of the Affordable Care Act, ensuring that claims are accurate, reimbursable, and protected against fraudulent billing [116]. In India, analogous obligations exist under the Digital Information Security in Healthcare Act (DISHA, proposed framework 2023), which mandates secure management, access control, and auditability of patient records, while international frameworks such as the General Data Protection Regulation (GDPR) regulate cross-border health data sharing. Despite its importance, clinical validation faces multiple challenges: inconsistent or fragmented documentation, lack of standardized diagnostic criteria, time-constrained workflows, and regulatory complexity. Studies suggest that up to 25% of hospital claims may be denied due to documentation gaps (Change Healthcare, 2020 [117]). Integrating compliance across multiple jurisdictions—HIPAA for US patient data, DISHA for Indian healthcare data, and GDPR for cross-border exchange—adds additional layers of operational and technical complexity. A tri-regulatory overlap map helps visualize these intersecting obligations. HIPAA primarily governs patient privacy, access, and record retention. DISHA focuses on data security, audit trails, and Indian jurisdiction compliance, and GDPR emphasizes cross-border data transfer and consent management. The overlapping challenges in clinical validation: Clinical validation is a post-claim forensic process in which licensed clinicians verify that diagnoses and procedure codes—such as ICD-10-CM and CPT—are supported by clinical evidence, including lab results, imaging, treatments, and progress notes. This process is mandated under HIPAA (1996) in the United States, enforced through the False Claims Act (31 U.S.C. §§ 3729–3733), and further reinforced via Section 6401(a) of the Affordable Care Act, ensuring that claims are accurate, reimbursable, and protected against fraudulent billing [116]. In India, analogous obligations exist under the Digital Information Security in Healthcare Act (DISHA, proposed framework 2023), which mandates secure management, access control, and auditability of patient records, while international frameworks such as the GDPR regulate cross-border health data sharing. Despite its importance, clinical validation faces multiple challenges: inconsistent or fragmented documentation, lack of standardized diagnostic criteria, time-constrained workflows, and regulatory complexity. Studies suggest that up to 25% of hospital claims may be denied due to documentation gaps (Change Healthcare, 2020 [117]). Integrating compliance across multiple jurisdictions—HIPAA for US patient data, DISHA for Indian healthcare data, and GDPR for cross-border exchange—adds additional layers of operational and technical complexity. A tri-regulatory overlap map helps visualize these intersecting obligations. HIPAA primarily governs patient privacy, access, and record retention. DISHA focuses on data security, audit trails, and Indian jurisdiction compliance, and GDPR emphasizes cross-border data transfer and consent management. The overlapping region in the map represents requirements that are common across all three frameworks, such as secure access, auditability, and patient consent for data use. Recognizing these intersections is crucial for healthcare providers, digital health platforms, and wearable device integrators, enabling them to design validation workflows that satisfy multiple regulations simultaneously, reducing the risk of penalties, data breaches, or claim denials while maintaining high data integrity.

2) Regulatory standards for wearables

Regulatory standards constitute the legally enforceable, systematically codified frameworks promulgated by national regulatory agencies and international standardization consortia, designed to ensure that wearable biosensors and digital health technologies adhere to validated benchmarks of clinical efficacy, safety, functional integrity, interoperability, and data stewardship. These frameworks extend across device classification heuristics, evidence-based risk stratification thresholds, electromagnetic compatibility (EMC) testing, software lifecycle validation, usability engineering, and post-market vigilance. At the global level, the core architecture of conformity assessment rests upon harmonized standards, including:

a. ISO 13485:2016 – Quality Management Systems for Medical Devices
b. ISO 14971 – Risk Management for Medical Devices
c. IEC 62304 – Software Lifecycle Processes
d. IEC 60601-1-2 – EMC Requirements for Medical Electrical Equipment
e. ISO/IEC 27001 and 27701 – Cybersecurity and Privacy Information Management

These standards are critical in regulatory filings, clinical trial design, dossier preparation, and lifecycle risk mitigation across jurisdictions [118]. In the United States, the US FDA governs wearable medical technologies under 21 CFR Parts 801–822, stratifying devices into Class I (low-risk), Class II (moderate-risk), and Class III (high-risk) categories [119]. Regulatory pathways include:

a. 510(k) premarket notification (substantial equivalence)
b. De Novo classification for novel, low-to-moderate risk devices
c. PMA (Premarket Approval) for Class III high-risk innovations

Devices must align with FDA-recognized consensus standards and adhere to cybersecurity guidelines issued under the NIST Cybersecurity Framework. Further, compliance with 21 CFR Part 803 mandates robust post-market surveillance and adverse event reporting [120]. Legal governance of personal health data falls under:

a. HIPAA (1996) – Ensuring confidentiality and integrity of Protected Health Information (PHI)
b. HITECH Act (2009) – Reinforcing breach notification mandates and health IT modernization

In the European Union, the Medical Device Regulation (EU MDR 2017/745) supersedes the earlier Major Depressive Disorder (MDD), demanding rigorous CE conformity assessment via Notified Bodies, including clinical performance evaluations, post-market clinical follow-up (PMCF), and traceability via Unique Device Identification [121]. For wearables collecting physiological data, GDPR (Regulation EU 2016/679) mandates compliance with data minimization, consent granularity, cross-border processing safeguards, and data subject rights [122]. In India, the regulatory landscape is delineated under the Medical Devices Rules, 2017 (amended 2020), administered by the Central Drugs Standard Control Organisation (CDSCO) [123]. Devices with diagnostic or therapeutic claims are classified into Class A–D under GSR 78(E) based on risk, triggering obligations for:

a. Medical Device Licensing
b. Technical Dossier Submission (including safety, effectiveness, and design control data)
c. Good Manufacturing Practices (Schedule 5)

For wireless-enabled devices, WPC ETA certification is mandated by the Department of Telecommunications. Safety compliance of electronic components is governed under the BIS CRS Scheme, specifically IS 13252 (Part 1):2010 for IT and medical electronics. The Digital Personal Data Protection (DPDP) Act 2023, modeled on GDPR principles, regulates digital consent architecture, breach notification timelines, and cross-border data flow governance [124]. At a supranational level, the International Medical Device Regulators Forum (IMDRF) promotes harmonization of device categorization, regulatory science best practices, and cross-border vigilance protocols. Concurrently, IEC TC 124 is pioneering standardization efforts in next-generation flexible bioelectronics, including textile-integrated sensors, stretchable circuits, and bioresorbable diagnostic systems—heralding a shift toward morphologically adaptive and seamlessly embedded medical technologies. Yet, despite the codified rigor of these frameworks, unresolved lacunae persist, particularly in the domain of software as a medical device, adaptive algorithms, and transnational data flows—areas where recent regulatory advisories have sought to impose more granular obligations.

a. Post-market vigilance: EU MDR PMCF (2021–2023 enforcement) – explicit obligation for periodic safety update reports for Class IIb/III wearables; India CDSCO GSR 102(E), 2020 – annual performance recertification for Class C/D devices with AI components.
b. Data governance conflicts: GDPR Art. 44–49 versus DPDP Act 2023, Sec. 16–17 – divergence on cross-border data transfer: GDPR requires adequacy decisions; DPDP requires "trusted geographies" notified by GoI. Cloud-hosted wearable datasets (AWS, Azure, GCP) are flagged as non-compliant under dual regimes.
c. Privacy and consent architecture: GDPR Recital 71 – explicit requirement for algorithmic transparency in automated decision-making; DPDP Act Sec. 7(2) – "consent managers" as fiduciaries, no equivalence in GDPR.
d. Cybersecurity enforcement: FDA 2023 (Cybersecurity in Medical Devices Guidance) – mandatory SBOM (Software Bill of Materials) submission for Class II/III wearables; EU MDR harmonized with IEC 81001,5,1 (2021) – secure product development lifecycle for health software.
e. Harmonization initiatives: IMDRF AI Principles (2023) – "Good Machine Learning Practices" (GMLP) codified; IEC TC124 WG10 (2024) – drafting safety standards for bioresorbable, textile-integrated sensors; WHO Global Digital Health Certification Network (GDHCN, 2023) – pilot frameworks for cross-border digital health device validation.

3) Regulatory ambiguity in SaMD classification

The landscape of Software as a Medical Device (SaMD) remains a regulatory twilight, where wellness-oriented applications blur into formally regulated medical technologies. The FDA's 2023 proposed AI/ML framework illuminates a pivotal distinction: "locked" algorithms, whose operational logic is fixed and immutable post-deployment, versus "adaptive" algorithms, which continuously evolve in response to real-world data streams. Mapping wearable neurotechnologies against this schema clarifies compliance pathways.

a. Case Example 1: Cognionics Quick-20 Headband – This device employs a 1D-CNN combined with LSTM networks to decode motor imagery signals from EEG electrodes. The neural decoding models are fully trained on pre-collected datasets and validated before deployment, with no real-time adaptation at the edge, classifying it as a locked algorithm. Its predictable performance ensures minimal post-deployment regulatory oversight.
b. Case Example 2: NeuroPace RNS System (Responsive Neurostimulation) – This seizure-detection wearable captures intracranial EEG signals and uses adaptive ML algorithms to detect pre-ictal patterns in real time. The model continuously updates its predictive parameters based on incoming EEG data, requiring robust change control plans, tiered risk management, independent multi-cohort validation, and potential recertification after significant algorithmic updates, exemplifying the regulatory demands of adaptive SaMD.

This evolving regulatory terrain is not without its shadows. Longitudinal performance drift remains uncharted for many edge-based neuro-wearables, limiting predictive certainty over extended use.

a. User compliance and data interpretation: Modern wearable health technologies are increasingly designed to integrate behavioral adherence mechanisms with advanced biosignal analytics for improved therapeutic outcomes. Devices like the Dexcom G7 feature factory-calibrated sensors, real-time hypoglycemia alerts, and algorithmic trend projections, with compliance supported through automated sensor replacement reminders [13]. The Abbott FreeStyle Libre 3 offers continuous glucose monitoring via a discreet, water-resistant sensor with haptic scan reminders, translating glycemic data into visual trend curves and predictive insight. Propeller Health's FDA-cleared inhaler sensors enable dose-tracking, issue medication-use reminders, and synchronize environmental data with symptom logs to generate individualized adherence analytics [125].

Table 7 provides a strategic compliance crosswalk for next-generation wearable health technologies, linking advanced functions—such as adaptive AI/ML, flexible bioelectronics, real-time decision support, and cross-border data handling—to the governing frameworks of EU MDR 2017/745, FDA statutes and guidances, and ISO/IEC standards. Beyond mere citation, it

Table 7
Compliance matrix for emerging wearable medical technologies

Emerging Wearable Function/Risk	EU MDR (Articles/Annexes)	FDA (Guidance/ Statutes)	ISO/IEC	Practical Compliance Actions
Adaptive AI/ML algorithms	Annex I GSPR; MDCG AI recommendations	FDA 2023 Proposed AI/ML Framework, Predetermined Change Control Plan	IMDRF GMLP; ISO 14971 risk management	Define adaptive vs. locked model; perform continuous monitoring; maintain documentation of algorithm updates; validate with independent datasets.
Cross-border cloud storage and multi-jurisdictional data flows	MDR + GDPR Art. 44–49 considerations	HIPAA and FDA data security guidance	ISO 27701 privacy info management	Map data flows; implement consent and lawful transfer mechanisms; ensure hosting aligns with national directives (DPDP/GDPR adequacy/SCC).
Textile-integrated and flexible bioelectronics	Annex I GSPR safety and performance	FDA guidance on novel device forms	IEC TC 124, ISO 13485	Conduct mechanical and electrical safety testing; document interoperability; verify performance under real-world mechanical stress; include in technical dossier.
Post-market AI performance monitoring	Art. 87–92 (vigilance); Annex III PMS	FDA post-market surveillance; 21 CFR Part 803	ISO 13485 §8, ISO/TR 20416	Implement AI performance drift detection; define thresholds for corrective actions; maintain logs for adaptive updates.
Interoperability with third-party platforms	Annex I GSPR	FDA interoperability guidance	IEC 62366,1, IEC 62304	Define API standards; validate data exchange and safety; maintain cybersecurity and access control for external integrations.
Dynamic risk re-classification due to software updates	Annex IX/X (conformity assessment)	FDA QMS and 21 CFR 820	ISO 14971 risk management	Establish a process for evaluating risk changes post-update; document change control and regulatory notification; integrate into QMS.
Wearable-driven real-time alerts and decision support	Annex I (safety, performance)	FDA Clinical Decision Support guidance	IEC 62304, ISO 62366	Validate alert thresholds; document human factors and usability; maintain clinical evidence for safety-critical notifications.
Emerging cybersecurity threats	Annex I (safety and security)	FDA Cybersecurity guidance	IEC 81001,5,1; ISO 27001	Threat modeling, penetration testing, patch management, SBOM documentation, incident response plans.

highlights actionable obligations for clinical validation, cybersecurity, interoperability, and post-market vigilance, offering a holistic roadmap for developers to navigate the regulatory labyrinth while ensuring global alignment and patient-safe innovation.

7. Future Perspectives

In the coming decade, smart wearables will evolve into bio-intelligent systems—soft, skin-adherent, and self-powered—designed to serve as continuous, real-time health sentinels. These devices will integrate multi-analyte electrochemical sensors embedded with nanomaterials like graphene, MXenes, and gold nanowires to detect metabolites (e.g., glucose, lactate, cortisol), electrolytes, and inflammatory markers in sweat, saliva, and interstitial fluid at nanomolar sensitivities. Flexible electrophysiological arrays will record biopotentials (ECG, EMG, EEG) with sub-1 μV noise, enabling on-skin cardiac and neurophysiological monitoring with diagnostic precision. Coupled with edge-based AI processors and drift, compensating algorithms, these systems will perform on-device inference, detecting early signs of arrhythmias, insulin resistance, or neurological events without cloud dependence. Thermoelectric and piezoelectric modules will harvest energy from body heat and motion, supporting autonomous operation for weeks. Standardized APIs (e.g., HL7 FHIR) will ensure seamless integration into EHRs, while federated learning architectures will enable model training across millions of devices without compromising data privacy. With digital twin frameworks, real-time biosensor inputs will merge with genomics and imaging data to simulate disease trajectories and personalize interventions.

Yet, two salient vulnerabilities demand explicit recognition. First, algorithmic bias remains an insidious constraint: a 2022 multi-country evaluation of FDA-cleared arrhythmia detection wearables (Apple Watch Series 6, Fitbit Sense) reported >95% sensitivity in controlled urban tertiary care environments, yet community-based deployments across rural India and sub-Saharan Africa revealed specificity declines to 78–82%. False arrhythmia alerts were disproportionately concentrated among darker-skinned individuals, reflecting inherent limitations of PPG under variable optical conditions. Geospatial stratification indicated that tribal and rural primary health center cohorts bore the brunt of misclassification, followed by semi-urban populations, whereas urban cohorts maintained consistently high fidelity. Contributing variables include constrained bandwidth, environmental noise, and heterogeneous skin pigmentation, interacting synergistically with device and algorithmic limitations. Conceptually, these deviations can be represented as a "supply heatmap" of error distribution, where darker shades signify districts with >20% false alerts,

Table 8
Global and Indian health data regulatory comparison for wearable healthcare devices

Regulatory Framework	Jurisdiction and Scope	Core Data Obligations	Cross-Regulatory Convergence	Distinctive Mandates
GDPR	European Union; personal and health data of EU residents	Granular consent, data minimization, transparency, right to access and erasure	Consent management, access controls, breach notification	Adequacy assessments for international data transfers
DPDP Act 2023	India: personal and health data of Indian citizens	Fiduciary consent management, breach notification, data localization, cross-border "trusted geographies"	Consent management, access controls, breach notification	Geographically restricted international data transfers
HIPAA	United States; Protected Health Information (PHI)	Privacy and security of PHI, breach reporting, compliance for covered entities and business associates	Security enforcement, breach reporting	PHI, specific safeguards, business associate accountability
DISHA (Proposed)	India: digital health and medical data governance	Secure storage, access control, auditability, and patient consent	Security enforcement, access control, and auditability	Mandatory digital health record audits, structured clinical data compliance

intermediate shading indicates 10–20%, and minimal shading reflects <10%. Study Table 8.

MXene production lifecycle assessment (LCA) depth (Ti_3C_2Tx via HF-based selective etching) generates fluoride-rich effluents with aquatic toxicity index >0.7, requires annealing at ≥900°C, and carries an estimated lifecycle carbon intensity of ~68 kg CO_2e per kg of MXene—nearly double that of equivalent quantities of GO. Reports from pilot LCA studies (2023, Helmholtz Zentrum, Germany) highlighted that MXene-derived sensor patches have a cradle-to-gate global warming potential (GWP) 3.5 times higher than conventional silicon-based microelectronics. By contrast, bio-based nanocellulose composites and silk fibroin substrates demonstrated GWP reductions of ~45% while maintaining comparable stretchability and dielectric stability. To reconcile eco-conscious claims, it is imperative to embed LCA into regulatory submissions, mandating disclosure of extraction, synthesis, deployment, and disposal footprints alongside conventional safety dossiers. As biodegradable substrates and self-healing electronics begin addressing environmental concerns, and regulatory advances establish wearable, specific safety and data ownership standards, these devices will no longer be auxiliary—they will become predictive, preventative health companions embedded in the very fabric of human life [126].

1) Scope 1 captures direct emissions from synthesis, heating, and HF handling.
2) Scope 2 captures indirect emissions from purchased electricity for etching, annealing, and fabrication.
3) Scope 3 includes all upstream and downstream supply chain emissions, for example, raw material extraction, chemical production, device logistics, and disposal.

Cradle-to-gate GWP (~3.5× conventional silicon electronics) is mainly dominated by the energy demand for annealing and etching. End-of-life emissions remain highly uncertain due to the limited recycling infrastructure for MXene-based devices.

Cradle-to-grave emission flow for Ti_3C_2Tx MXene production and use:

1) **Raw material extraction (cradle phase)**
   a. **Input:** Titanium (Ti), aluminum (Al), and carbon precursors (MAX phase: Ti_3AlC_2)
   b. **Processes:** Mining, refining, and precursor synthesis
   c. **Main emissions (Scope 3):**
      • Mining and transport of Ti and Al ores → CO_2, SO_2, NO_x
      • Chemical precursor manufacturing → Process off-gases, waste acids
   d. **Impact:** ~15–20% of total carbon footprint
   e. **Note:** High material intensity and long transport chains add to upstream emissions.

2) **MXene synthesis and etching (gate-to-factory phase)**
   a. **Input:** MAX phase powder, hydrofluoric acid (HF), deionized water, etching reactors
   b. **Processes:** HF-based selective etching removes the Al layer, yielding Ti_3C_2Tx flakes
   c. **Main emissions (Scope 1 and 2):**
      • Scope 1 (Direct):
        • HF handling → F-rich liquid effluents (aquatic toxicity index > 0.7)
        • Chemical vapors and local energy combustion emissions
      • Scope 2 (Indirect):
        • Electricity for etching, stirring, drying → CO_2 from power grids
   d. **Impact:** ~35–40% of total GWP
   e. **Highlight:** High chemical hazard and treatment load drive the ecotoxicity footprint.

3) **Thermal annealing and post-processing**
   a. **Input:** Synthesized Ti_3C_2Tx, inert gas environment
   b. **Processes:** Annealing ≥ 900°C to stabilize surface terminations and conductivity
   c. **Main emissions (Scope 2):**

- Electricity and/or natural gas for furnaces → High CO_2e output

d. **Impact:** ~30–35% of GWP
e. **Note:** Energy demand during this step nearly doubles the total carbon intensity compared to GO.

4) **Device fabrication and assembly**
   a. **Input:** MXene inks/films, polymer or silk fibroin substrates, micro-patterning tools
   b. **Processes:** Printing, deposition, encapsulation, curing
   c. **Main emissions (Scope 2 and 3):**
      - Equipment power usage
      - Solvent volatilization and substrate manufacturing emissions
   d. **Impact:** ~10% of total GWP
   e. **Insight:** Bio-based substrates (e.g., nanocellulose, silk fibroin) reduce GWP by ~45%.
5) **Device use phase**
   a. **Input:** Energy for wearable operation (battery charging, data transfer)
   b. **Main emissions (Scope 2):**
      - Indirect CO_2e from electricity consumption during active use
   c. **Impact:** Minor (~3–5%) but cumulative over device lifespan
   d. **Note:** Longer operational life reduces per-use environmental cost.

6) **End-of-life and disposal (grave phase)**
   a. **Processes:** Waste collection, incineration, or landfill
   b. **Main emissions (Scope 3):**
      - Uncertain due to a lack of MXene recycling infrastructure
      - Potential fluoride leaching, heavy-metal release, or incomplete combustion residues
   c. **Impact:** Environmentally risky but poorly quantified
   d. **Future direction:** Design for recyclability and biodegradable hybrid composites.

As bio-intelligent wearables evolve into continuous, real-time health sentinels, their transformative potential must be matched by a steadfast commitment to ethical deployment. At the heart of this commitment lies human autonomy and dignity: users must retain full control over their data, devices, and engagement with AI-driven insights, empowering informed choices rather than passive monitoring. Equally critical is fairness and nondiscrimination; the algorithms guiding these wearables should be trained on diverse datasets that reflect the full spectrum of age, sex, ethnicity, SES, and occupational backgrounds, ensuring equitable access and unbiased clinical decision-making. Transparency and explainability serve as the bridge between complex AI inference and human understanding, enabling users and clinicians to interpret predictions and understand the rationale behind alerts or recommendations. Privacy and data security form the protective backbone, with encrypted communications, federated learning, and on-device computation safeguarding intimate biometric and health information. In parallel, accountability and responsibility establish clear lines of liability for AI-driven decisions, while safety and well-being demand rigorous validation, real-world testing, and continuous performance monitoring to ensure reliability under dynamic physiological and environmental conditions. Finally, embedding principles of sustainability and eco-conscious design ensures that the march of innovation does not come at the expense of the planet.

Ethical Statement

This study does not contain any studies with human or animal subjects performed by any of the authors.

Conflicts of Interest

The authors declare that they have no conflicts of interest to this work.

Data Availability Statement

Data are available from the corresponding author upon reasonable request.

Author Contribution Statement

Simranjit Kaur: Conceptualization, Methodology, Investigation, Resources, Data curation, Writing – original draft. **Tania Acharjee:** Conceptualization, Formal analysis, Investigation, Resources, Writing – original draft, Writing – review & editing, Project administration. **Debashree Das:** Methodology, Resources. **Monika Bhatia:** Validation, Formal analysis, Data curation. **Sushman Sharma:** Validation, Visualization. **Ashish Patel:** Validation, Visualization. **Dinesh Bhatia:** Conceptualization, Methodology, Validation, Data curation, Writing – review & editing, Visualization, Supervision, Project administration.

References

[1] Adner, R., & Levinthal, D. (2001). Demand heterogeneity and technology evolution: Implications for product and process innovation. *Management Science*, *47*(5), 611–628. https://doi.org/10.1287/mnsc.47.5.611.10482

[2] Gao, Y., Li, H., & Luo, Y. (2015). An empirical study of wearable technology acceptance in healthcare. *Industrial Management & Data Systems*, *115*(9), 1704–1723. https://doi.org/10.1108/IMDS-03-2015-0087

[3] Tavakoli, M., Carriere, J., & Torabi, A. (2020). Robotics, smart wearable technologies, and autonomous intelligent systems for healthcare during the COVID-19 pandemic: An analysis of the state of the art and future vision. *Advanced Intelligent Systems*, *2*(7), 2000071. https://doi.org/10.1002/aisy.202000071

[4] Hernandez-Silveira, M., Ahmed, K., Ang, S. S., Zandari, F., Mehta, T., Weir, R., . . . , & Brett, S. J. (2015). Assessment of the feasibility of an ultra-low power, wireless digital patch for the continuous ambulatory monitoring of vital signs. *BMJ Open*, *5*(5), e006606. https://doi.org/10.1136/bmjopen-2014-006606

[5] Zhang, T., Yu, Y., Lu, Y., Tang, H., Chen, K., Shi, J., . . . , & Zheng, Y. (2026). Bridging biodegradable metals and biodegradable polymers: A comprehensive review of biodegradable metal–organic frameworks for biomedical application. *Progress in Materials Science*, *155*, 101526. https://doi.org/10.1016/j.pmatsci.2025.101526

[6] Hansen, L., & Nissenbaum, H. (2009). Digital disaster, cyber security, and the Copenhagen School. *International Studies Quarterly*, *53*(4), 1155–1175. https://doi.org/10.1111/j.1468-2478.2009.00572.x

[7] Kim, D. H., Lu, N., Ma, R., Kim, Y. S., Kim, R. H., Wang, S., . . . , & Rogers, J. A. (2011). Epidermal electronics. *Science*, *333*(6044), 838–843. https://doi.org/10.1126/science.1206157

[8] Tee, B. C.-K., Wang, C., Allen, R., & Bao, Z. (2012). An electrically and mechanically self-healing composite with pressure-and flexion-sensitive properties for electronic skin applications. *Nature Nanotechnology*, *7*(12), 825–832. https://doi.org/10.1038/nnano.2012.192

[9] Kaur, P., Dhir, A., Chen, S., & Rajala, R. (2020). Understanding online regret experience using the theoretical lens of flow experience. *Computers in Human Behavior*, *57*, 230–239. https://doi.org/10.1016/j.chb.2015.12.041

[10] Rana, R. K., Kapoor, N., Kumar, D., Verma, M., & Taneja, G. (2024). Digital health revolution in India: Transforming health and medicine. *Indian Journal of Community Medicine*, *49*(Suppl 2), S205–S209. https://doi.org/10.4103/ijcm.ijcm_803_24

[11] Kapogianni, N. A., Sideraki, A., & Anagnostopoulos, C. N. (2025). Using smartwatches in stress management, mental health, and well-being: A systematic review. *Algorithms*, *18*(7), 419. https://doi.org/10.3390/a18070419

[12] Mishra, U. S., Yadav, S., & Joe, W. (2024). The Ayushman Bharat digital mission of India: An assessment. *Health Systems & Reform*, *10*(2), 2392290. https://doi.org/10.1080/23288604.2024.2392290

[13] Hanson, K., Kipnes, M., & Tran, H. (2024). Comparison of point accuracy between two widely used continuous glucose monitoring systems. *Journal of Diabetes Science and Technology*, *18*(3), 598–607. https://doi.org/10.1177/19322968231225676

[14] Lee, M. A., Song, M., Bessette, H., Davis, M. R., Tyner, T. E., & Reid, A. (2023). Use of wearables for monitoring cardiometabolic health: A systematic review. *International Journal of Medical Informatics*, *179*, 105218. https://doi.org/10.1016/j.ijmedinf.2023.105218

[15] Vo, D. K., & Trinh, K. T. L. (2024). Advances in wearable biosensors for healthcare: Current trends, applications, and future perspectives. *Biosensors*, *14*(11), 560. https://doi.org/10.3390/bios14110560

[16] Klier, K., Koch, L., Graf, L., Schinköthe, T., & Schmidt, A. (2023). Diagnostic accuracy of single-lead electrocardiograms using the Kardia Mobile App and the Apple Watch 4: Validation study. *JMIR Cardio*, *7*, e50701. https://doi.org/10.2196/50701

[17] Ronca, V., Martinez-Levy, A. C., Vozzi, A., Giorgi, A., Aricò, P., Capotorto, R., . . . , & di Flumeri, G. (2023). Wearable technologies for electrodermal and cardiac activity measurements: A comparison between Fitbit Sense, Empatica E4 and Shimmer GSR3+. *Sensors*, *23*(13), 5847. https://doi.org/10.3390/s23135847

[18] Didyuk, O., Econom, N., Guardia, A., Livingston, K., & Klueh, U. (2021). Continuous glucose monitoring devices: Past, present, and future focus on the history and evolution of technological innovation. *Journal of Diabetes Science and Technology*, *15*(3), 676–683. https://doi.org/10.1177/1932296819899394

[19] Montes, J., Young, J. C., Tandy, R., & Navalta, J. W. (2018). Reliability and validation of the Hexoskin wearable bio-collection device during walking conditions. *International Journal of Exercise Science*, *11*(7), 806–816. https://doi.org/10.70252/YPHF4748

[20] Lee, S. P., Aranyosi, A. J., & Ghaffari, R. (2025). Wearable electrochemical biosensors for remote hydration and health management. *Nature Reviews Electrical Engineering*, *2*(6), 371–372. https://doi.org/10.1038/s44287-025-00184-4

[21] Chazal, E., Parmentier, A. L., Pili-Floury, S., Bouhaddi, M., Borot, S., Perrotti, A., . . . , & du Mont, L. S. (2022). Perioperative blood glucose variability and autonomic nervous system activity in on-pump cardiac surgery patients: Study protocol of a single-center observational study. *Medicine*, *101*(47), e31821. https://doi.org/10.1097/md.0000000000031821

[22] Patel, V., Chesmore, A., Legner, C. M., & Pandey, S. (2022). Trends in workplace wearable technologies and connected-worker solutions for next-generation occupational safety, health, and productivity. *Advanced Intelligent Systems*, *4*(1), 2100099. https://doi.org/10.1002/aisy.202100099

[23] O'Grady, B., Lambe, R., Baldwin, M., Acheson, T., & Doherty, C. (2024). The validity of Apple Watch Series 9 and Ultra 2 for serial measurements of heart rate variability and resting heart rate. *Sensors*, *24*(19), 6220. https://doi.org/10.3390/s24196220

[24] Koohang, A., Nord, J. H., Ooi, K., Tan, G. W., Al-Emran, M., Aw, E. C., . . . , & Wong, L. (2023). Shaping the metaverse into reality: A holistic multidisciplinary understanding of opportunities, challenges, and avenues for future investigation. *Journal of Computer Information Systems*, *63*(3), 735–765. https://doi.org/10.1080/08874417.2023.2165197

[25] Scholes, R. E., & Rabkin, E. S. (1977). *Science fiction: History-science-vision*. UK: Oxford University Press.

[26] Schneegass, S., Olsson, T., Mayer, S., & van Laerhoven, K. (2016). Mobile interactions augmented by wearable computing: A design space and vision. *International Journal of Mobile Human Computer Interaction*, *8*(4), 104–114. https://doi.org/10.4018/ijmhci.2016100106

[27] Kennedy, H. L. (2006). The history, science, and innovation of Holter technology. *Annals of Noninvasive Electrocardiology*, *11*(1), 85–94. https://doi.org/10.1111/j.1542-474X.2006.00067.x

[28] Tudor-Locke, C., & Bassett, D. R. (2004). How many steps/day are enough? Preliminary pedometer indices for public health. *Sports Medicine*, *34*(1), 1–8. https://doi.org/10.2165/00007256-200434010-00001

[29] Park, S. M., & Kim, Y. G. (2022). A metaverse: Taxonomy, components, applications, and open challenges. *IEEE Access*, *10*, 4209–4251. https://doi.org/10.1109/ACCESS.2021.3140175

[30] Paulino, N., & Pessoa, L. M. (2022). Self-localization via circular Bluetooth 5.1 antenna array receiver. *IEEE Access*, *11*, 365–395. https://doi.org/10.1109/ACCESS.2022.3233130

[31] Wang, Z., Zhao, X., Yan, K., Zhang, P., Zhang, S., & Fan, H. (2025). Smart textiles for chronic disease management: Advancements, applications, and future prospects. *Materials Science and Engineering R Reports*, *164*, 100987. https://doi.org/10.1016/j.mser.2025.100987

[32] Davoudi, A., Urbanek, J. K., Etzkorn, L., Parikh, R., Soliman, E. Z., Wanigatunga, A. A., . . . , & Chen, L. Y. (2024). Validation of a Zio XT patch accelerometer for the objective assessment of physical activity in the Atherosclerosis Risk in Communities (ARIC) study. *Sensors*, *24*(3), 761. https://doi.org/10.3390/s24030761

[33] Kumar, H., Bhaidasna, H., & Patel, K. (2025). Always on, always exposed: Survey on Bluetooth risks in wearable devices. *IET Conference Proceedings*, *2025*(7), 300–306. https://doi.org/10.1049/icp.2025.1310

[34] Frank, L. R., Galinsky, V. L., Krigolson, O., Tapert, S., Bickel, S., & Martinez, A. (2025). Imaging of brain electric field networks with spatially resolved EEG. *eLife*, *13*, RP100123. https://doi.org/10.7554/eLife.100123.3

[35] van Rheden, V., Harbour, E., Finkenzeller, T., & Meschtscherjakov, A. (2024). Into the rhythm: Evaluating breathing instruction sound experiences on the run with novice female runners. *Multimodal Technologies and Interaction*, *8*(4), 25. https://doi.org/10.3390/mti8040025
[36] Man, S., Maan, A. C., Schalij, M. J., & Swenne, C. A. (2015). Vectorcardiographic diagnostic & prognostic information derived from the 12-lead electrocardiogram: Historical review and clinical perspective. *Journal of Electrocardiology*, *48*(4), 463–475. https://doi.org/10.1016/j.jelectrocard.2015.05.002
[37] Tierney, M., Adeyemi, E. O., & Bommer, S. (2025). A systematic literature review: Cognitive workload assessment in human factors research. *Advances in Human-Computer Interaction*, *2025*(1), 9313239. https://doi.org/10.1155/ahci/9313239
[38] Bhullar, K. K., & Singh, N. (2024). From concept to cure: The life and legacy of Scipione Riva-Rocci. *Cureus*, *16*(9), e70436. https://doi.org/10.7759/cureus.70436
[39] Roguin, A. (2006). Rene Theophile Hyacinthe Laënnec (1781–1826): The man behind the stethoscope. *Clinical Medicine & Research*, *4*(3), 230–235. https://doi.org/10.3121/cmr.4.3.230
[40] Mandal, N. G. (2006). Respirometers including spirometer, pneumotachograph and peak flow meter. *Anaesthesia & Intensive Care Medicine*, *7*(1), 1–5. https://doi.org/10.1383/anes.2006.7.1.1
[41] Albayati, M. G., Dano, E. B., Rajamani, R., & Thompson, A. E. (2023). A model-based engineering approach for evaluating software-defined radio architecture. *Systems*, *11*(9), 480. https://doi.org/10.3390/systems11090480
[42] Dearing, C. G., & Paton, C. D. (2023). Is Stryd critical power a meaningful parameter for runners? *Biology of Sport*, *40*(3), 657–664. https://doi.org/10.5114/biolsport.2023.118025
[43] Guarducci, S., Jayousi, S., Caputo, S., & Mucchi, L. (2025). Key fundamentals and examples of sensors for human health: Wearable, non-continuous, and non-contact monitoring devices. *Sensors*, *25*(2), 556. https://doi.org/10.3390/s25020556
[44] Swetha, L., & Muneeswari, G. (2016). A survey on wearable computers: Human computer interface. In *Proceedings of the International Conference on Informatics and Analytics*, 23. https://doi.org/10.1145/2980258.2980305
[45] Lopes, J. M., Silva, L. F., Massano-Cardoso, I., & Galhardo, A. (2025). Running towards a better brand attitude: How gamification in Nike Run Club can help? *Journal of the Knowledge Economy*, *16*(4), 15427–15455. https://doi.org/10.1007/s13132-024-02398-7
[46] Bravo-Zanoguera, M., Cuevas-González, D., Reyna, M. A., García-Vázquez, J. P., & Avitia, R. L. (2020). Fabricating a portable ECG device using AD823X analog front-end microchips and open-source development validation. *Sensors*, *20*(20), 5962. https://doi.org/10.3390/s20205962
[47] Cornett, J., O'Grady, A., Vouaillat, A., Michaud, J., Muret, F., Weatherholtz, W., . . . , & Galchev, T. (2018). Continuous machine health monitoring enabled through self-powered embedded intelligence and communication. *Journal of Physics: Conference Series*, *1052*(1), 012025. https://doi.org/10.1088/1742-6596/1052/1/012025
[48] Backiyalakshmi, G., Snekhalatha, U., & Salvador, A. L. (2024). Recent advancements in non-invasive wearable electrochemical biosensors for biomarker analysis–A review. *Analytical Biochemistry*, *692*, 115578. https://doi.org/10.1016/j.ab.2024.115578
[49] Fung, E., Järvelin, M. R., Doshi, R. N., Shinbane, J. S., Carlson, S. K., Grazette, L. P., . . . , & Peters, N. S. (2015). Electrocardiographic patch devices and contemporary wireless cardiac monitoring. *Frontiers in Physiology*, *6*, 149. https://doi.org/10.3389/fphys.2015.00149
[50] Wang, Y., Tang, Y., Wang, Q., Ge, M., Wang, J., Cui, X., . . . , & Xu, S. (2025). Advances in brain computer interface for amyotrophic lateral sclerosis communication. *Brain-X*, *3*(1), e70023. https://doi.org/10.1002/brx2.70023
[51] Stanković, M., Hu, X., Ozer, A. A., & Karabiyik, U. (2025). How engaged are you? A forensic analysis of the Oura Ring Gen 3 application across iOS, Android, and Cloud platforms. *International Journal of Information Security*, *24*(1), 24. https://doi.org/10.1007/s10207-024-00936-7
[52] Zhou, S., Brady, B., & Anstey, K. J. (2025). Criterion validity of five open-source app-based cognitive and sensory tasks in an Australian adult life course sample aged 18 to 82: Labs without walls. *Behavior Research Methods*, *57*(2), 69. https://doi.org/10.3758/s13428-024-02583-1
[53] Zhou, L., Chen, S., Liu, J., Zhou, Z., Yan, Z., Li, C., . . . , & Li, Z. A. (2025). When artificial intelligence (AI) meets organoids and organs-on-chips (OoCs): Game-changer for drug discovery and development. *The Innovation Life*, *3*(1), 100115. https://doi.org/10.59717/j.xinn-life.2024.100115
[54] Obianyo, C., Ezeamii, V. C., Idoko, B., Adeyinka, T., Ejembi, E. V., Idoko, J. E., . . . , & Ugwu, O. J. (2024). The future of wearable health technology: From monitoring to preventive healthcare. *World Journal of Biology Pharmacy and Health Sciences*, *20*(1), 36–55. https://doi.org/10.30574/wjbphs.2024.20.1.0709
[55] Rawal, K., Acharya, A., & Soni, S. (2025). Embracing technological advancements: The transformation of healthcare services in the digital age. In C. Saini, N. Gupta, & A. Kumar (Eds.), *Handbook of disruptive technologies: Operations, business, management, and healthcare* (pp. 174–186). CRC Press. https://doi.org/10.1201/9781032700953-14
[56] Lin, J., Peng, Z., Liu, Y., Ruiz-Zepeda, F., Ye, R., Samuel, E. L., . . . , & Tour, J. M. (2014). Laser-induced porous graphene films from commercial polymers. *Nature Communications*, *5*(1), 5714. https://doi.org/10.1038/ncomms6714
[57] Bensalah, F., Pézard, J., Haddour, N., Erouel, M., Buret, F., & Khirouni, K. (2021). Carbon nano-fiber/PDMS composite used as corrosion-resistant coating for copper anodes in microbial fuel cells. *Nanomaterials*, *11*(11), 3144. https://doi.org/10.3390/nano11113144
[58] Krishna Prasad, N. V., Venkata Prasad, K., Ramesh, S., Phanidhar, S. V., Venkata Ratnam, K., Janardhan, S., . . . , & Srinivas, K. (2020). Ceramic sensors: A mini-review of their applications. *Frontiers in Materials*, *7*, 593342. https://doi.org/10.3389/fmats.2020.593342
[59] Neri, L., Oberdier, M. T., van Abeelen, K. C., Menghini, L., Tumarkin, E., Tripathi, H., . . . , & Halperin, H. R. (2023). Electrocardiogram monitoring wearable devices and artificial-intelligence-enabled diagnostic capabilities: A review. *Sensors*, *23*(10), 4805. https://doi.org/10.3390/s23104805
[60] Cosoli, G., Spinsante, S., Scardulla, F., D'Acquisto, L., & Scalise, L. (2021). Wireless ECG and cardiac monitoring systems: State of the art, available commercial devices and useful electronic components. *Measurement*, *177*, 109243. https://doi.org/10.1016/j.measurement.2021.109243
[61] Lee, M. B., Kramer, D. R., Peng, T., Barbaro, M. F., Liu, C. Y., Kellis, S., & Lee, B. (2019). Clinical neuroprosthetics: Today and tomorrow. *Journal of Clinical Neuroscience*, *68*, 13–19. https://doi.org/10.1016/j.jocn.2019.07.056
[62] Zhou, L., Guess, M., Kim, K. R., & Yeo, W. H. (2024). Skin-interfacing wearable biosensors for smart health monitoring of

infants and neonates. *Communications Materials*, *5*(1), 72. https://doi.org/10.1038/s43246-024-00511-6

[63] Scardulla, F., Cosoli, G., Spinsante, S., Poli, A., Iadarola, G., Pernice, R., ..., & D'Acquisto, L. (2023). Photoplethysmograhic sensors, potential and limitations: Is it time for regulation? A comprehensive review. *Measurement*, *218*, 113150. https://doi.org/10.1016/j.measurement.2023.113150

[64] Wang, Y., Shen, N., Zhu, Z., Liu, J., Qi, X., Liu, Z., ..., & Xiang, H. (2025). Electrospun 3D nanofibrous materials and their applications in orthopaedics. *Advanced Composites and Hybrid Materials*, *8*(1), 62. https://doi.org/10.1007/s42114-024-01120-0

[65] Fink, P. L., Sayem, A. S. M., Teay, S. H., Ahmad, F., Shahariar, H., & Albarbar, A. (2021). Development and wearer trial of ECG-garment with textile-based dry electrodes. *Sensors and Actuators A: Physical*, *328*, 112784. https://doi.org/10.1016/j.sna.2021.112784

[66] Sahud, H., Berger, R. P., Hamm, M., Heineman, E., Cameron, F., Wasilewski, J., ..., & Muniz, G. B. (2025). Understanding parental choices related to infant sleep practices in the United States using a mixed methods approach. *BMC Pediatrics*, *25*(1), 9. https://doi.org/10.1186/s12887-024-05332-7

[67] Lospinoso, D., Colombelli, A., Pal, S., Cretì, P., Martucci, M. C., Giancane, G., ..., & Manera, M. G. (2025). Sustainable and flexible surface-enhanced Raman scattering transducer: Gold nanoparticle-bacterial cellulose composite for pesticide monitoring in agrifood systems. *Biosensors*, *15*(2), 69. https://doi.org/10.3390/bios15020069

[68] Vimalanathan, B., Thiyagarajan, D., Mary, R. N., Sachidanandam, M., Ignacimuthu, S., Gnanasampanthapandian, D., ..., & Palaniyandi, K. (2025). Composites of reduced graphene oxide based on silver nanoparticles and their effect on breast cancer stem cells. *Bioengineering*, *12*(5), 508. https://doi.org/10.3390/bioengineering12050508

[69] Peng, Y., Huang, H., Liu, H., Dong, J., Zhang, Y., Long, J., & Huang, Y. (2025). Robust triboelectric e-textile with semi-bonded bilayers for on-skin thermal regulation and self-powered motion monitoring. *Advanced Fiber Materials*, *7*(4), 1165–1176. https://doi.org/10.1007/s42765-025-00546-5

[70] Tseghai, G. B., Mengistie, D. A., Malengier, B., Fante, K. A., & van Langenhove, L. (2020). PEDOT: PSS-based conductive textiles and their applications. *Sensors*, *20*(7), 1881. https://doi.org/10.3390/s20071881

[71] Zhao, X., Yang, J., Zhao, Y., Zhai, W., Zhou, K., Zheng, G., ..., & Shen, C. (2024). Flexible pressure sensor based on CNTs/CB/PDMS sponge with porous and microdome structures for sitting posture discrimination. *Chemical Engineering Journal*, *502*, 157878. https://doi.org/10.1016/j.cej.2024.157878

[72] Kurra, N., Jiang, Q., Nayak, P., & Alshareef, H. N. (2019). Laser-derived graphene: A three-dimensional printed graphene electrode and its emerging applications. *Nano Today*, *24*, 81–102. https://doi.org/10.1016/j.nantod.2018.12.003

[73] Jiang, N., Chen, G., Zhou, F., Ma, B., Zhao, C., & Liu, H. (2024). A dual-mode wearable sensor with electrophysiological and pressure sensing for cuffless blood pressure monitoring. *Journal of Materials Chemistry C*, *12*(39), 15915–15923. https://doi.org/10.1039/d4tc02494j

[74] Phan, D. T., Phan, T. T. V., Huynh, T. C., Park, S., Choi, J., & Oh, J. (2022). Noninvasive, wearable multi biosensors for continuous, long-term monitoring of blood pressure via internet of things applications. *Computers and Electrical Engineering*, *102*, 108187. https://doi.org/10.1016/j.compeleceng.2022.108187

[75] Zhang, Y., Querney, J., Subramani, Y., Naismith, K., Singh, P., Fochesato, L. A., ..., & Nagappa, M. (2025). Biobeat monitor utilization in various healthcare settings: A systematic review. *Digital Health*, *11*, 20552076251324012. https://doi.org/10.1177/20552076251324012

[76] Yu, S., Sun, X., Liu, J., & Li, S. (2024). OECT-Inspired electrical detection. *Talanta*, *275*, 126180. https://doi.org/10.1016/j.talanta.2024.126180

[77] Keene, S. T., Fogarty, D., Cooke, R., Casadevall, C. D., Salleo, A., & Parlak, O. (2019). Wearable organic electrochemical transistor patch for multiplexed sensing of calcium and ammonium ions from human perspiration. *Advanced Healthcare Materials*, *8*(24), 1901321. https://doi.org/10.1002/adhm.201901321

[78] Dubey, H., Goldberg, J. C., Abtahi, M., Mahler, L., & Mankodiya, K. (2015). EchoWear: Smartwatch technology for voice and speech treatments of patients with Parkinson's disease. In *Proceedings of the Conference on Wireless Health*, 15. https://doi.org/10.1145/2811780.2811957

[79] Yu, Y., Liao, X., & Feng, W. (2025). Recent development of elastomer-based smart sensing materials and structures. *Advanced Composites and Hybrid Materials*, *8*(1), 138. https://doi.org/10.1007/s42114-024-01168-y

[80] Bergenstal, R. M., Klonoff, D. C., Garg, S. K., Bode, B. W., Meredith, M., Slover, R. H., ..., & Kaufman, F. R. (2013). Threshold-based insulin-pump interruption for reduction of hypoglycemia. *New England Journal of Medicine*, *369*(3), 224–232. https://doi.org/10.1056/NEJMoa1303576

[81] Shi, Y., Zhang, Z., Huang, Q., Lin, Y., & Zheng, Z. (2023). Wearable sweat biosensors on textiles for health monitoring. *Journal of Semiconductors*, *44*(2), 021601. https://doi.org/10.1088/1674-4926/44/2/021601

[82] Su, H., Usman, K. A. S., Nilghaz, A., Bu, Y., Tang, K., Dai, L., ..., & Li, J. (2024). Efficient energy generation from a sweat-powered, wearable, MXene-based hydroelectric nanogenerator. *Device*, *2*(5), 100356. https://doi.org/10.1016/j.device.2024.100356

[83] Singh, A. N., & Nam, K. W. (2025). Gel-based self-powered nanogenerators: Materials, mechanisms, and emerging opportunities. *Gels*, *11*(6), 451. https://doi.org/10.3390/gels11060451

[84] Han, Y. Q., Lei, Z. Y., & Wu, P. Y. (2025). MXene nanosheet-enhanced ionotronic hydrogels for wireless powering and noncontact sensing. *Chinese Journal of Polymer Science*, *43*(4), 572–580. https://doi.org/10.1007/s10118-025-3253-6

[85] Yusuf, A. A., Nwobodo-Nzeribe, N. H., Eze-Steven, P., & Nwabueze, C. N. (2025). Design and implementation of portable low-cost heart rate monitoring ECG system. *Engineering and Technology Journal*, *10*(1), 3487–3492. https://doi.org/10.47191/etj/v10i01.05

[86] Cay, G., Solanki, D., Al Rumon, M. A., Ravichandran, V., Fapohunda, K. O., & Mankodiya, K. (2024). SolunumWear: A smart textile system for dynamic respiration monitoring across various postures. *iScience*, *27*(7), 110223. https://doi.org/10.1016/j.isci.2024.110223

[87] Hu, Q., Zhang, Q., Lu, H., Wu, S., Zhou, Y., Huang, Q., ..., & Zhao, N. (2024). Contactless arterial blood pressure waveform monitoring with mmwave radar. In *Proceedings*

of the ACM on Interactive, Mobile, Wearable and Ubiquitous Technologies, *8*(4), 178. https://doi.org/10.1145/3699781

[88] Kedambaimoole, V., Harsh, K., Rajanna, K., Sen, P., Nayak, M. M., & Kumar, S. (2022). MXene wearables: Properties, fabrication strategies, sensing mechanism and applications. *Materials Advances*, *3*(9), 3784–3808. https://doi.org/10.1039/D1MA01170G

[89] Lee, S., Ho, D. H., Jekal, J., Cho, S. Y., Choi, Y. J., Oh, S., …, & Cho, J. H. (2024). Fabric-based lamina emergent MXene-based electrode for electrophysiological monitoring. *Nature Communications*, *15*(1), 5974. https://doi.org/10.1038/s41467-024-49939-x

[90] Kabiri Ameri, S., Ho, R., Jang, H., Tao, L., Wang, Y., Wang, L., …, & Lu, N. (2017). Graphene electronic tattoo sensors. *ACS Nano*, *11*(8), 7634–7641. https://doi.org/10.1021/acsnano.7b02182

[91] Moein, A., Malekmohammadi, M., & Youssefi, K. (2010). An introduction to the next generation of radiology in the Web 2.0 world. In *26th Southern Biomedical Engineering Conference*, 459–462. https://doi.org/10.1007/978-3-642-14998-6_117

[92] Pang, C., Koo, J. H., Nguyen, A., Caves, J. M., Kim, M. G., Chortos, A., …, & Bao, Z. (2015). Highly skin-conformal microhairy sensor for pulse signal amplification. *Advanced Materials*, *27*(4), 634–640. https://doi.org/10.1002/adma.201403807

[93] Lee, K., Kim, T., Im, S., Lee, Y. J., Jeong, S., Shin, H., …, & Lee, S. H. (2025). A wearable stethoscope for accurate real-time lung sound monitoring and automatic wheezing detection based on an AI algorithm. *Engineering, 53*, 116–129. https://doi.org/10.1016/j.eng.2024.12.031

[94] Tao, D., Su, P., Chen, A., Gu, D., Eginligil, M., & Huang, W. (2025). Electro-spun nanofibers-based triboelectric nanogenerators in wearable electronics: Status and perspectives. *npj Flexible Electronics*, *9*(1), 4. https://doi.org/10.1038/s41528-024-00357-5

[95] Zhang, Q., Soham, D., Liang, Z., & Wan, J. (2025). Advances in wearable energy storage and harvesting systems. *Med-X*, *3*(1), 3. https://doi.org/10.1007/s44258-024-00048-w

[96] Li, Y., Sun, Y., Lu, Q., Lu, Y., & Kong, D. (2024). Recent advances in stretchable and permeable electrodes for epidermal electronics. *Advanced Sensor Research*, *3*(6), 2300195. https://doi.org/10.1002/adsr.202300195

[97] Barja, A. M., Ryu, Y. K., Tarancón, S., Tejado, E., Hamada, A., Velasco, A., & Martinez, J. (2024). Laser-induced graphene strain sensors for body movement monitoring. *ACS Omega*, *9*(37), 38359–38370. https://doi.org/10.1021/acsomega.3c09067

[98] Park, S., Han, C. H., & Im, C. H. (2020). Design of wearable EEG devices specialized for passive brain–computer interface applications. *Sensors*, *20*(16), 4572. https://doi.org/10.3390/s20164572

[99] Sugden, R. J., Pham-Kim-Nghiem-Phu, V. L. L., Campbell, I., Leon, A., & Diamandis, P. (2023). Remote collection of electrophysiological data with brain wearables: Opportunities and challenges. *Bioelectronic Medicine*, *9*(1), 12. https://doi.org/10.1186/s42234-023-00114-5

[100] Choudhury, D., & Hussain, M. F. (2021). Neoproterozoic highly fractionated I-type granitoids of Shillong Plateau, Meghalaya, Northeast India: Geochemical constraints on their petrogenesis. *Acta Geochimica*, *40*(1), 51–66. https://doi.org/10.1007/s11631-020-00410-w

[101] Shin, J. W., Kim, D. J., Jang, T. M., Han, W. B., Lee, J. H., Ko, G. J., …, & Hwang, S. W. (2024). Highly elastic, bioresorbable polymeric materials for stretchable, transient electronic systems. *Nano-Micro Letters*, *16*(1), 102. https://doi.org/10.1007/s40820-023-01268-2

[102] Zhao, Y., Zhang, Y., Liu, Z., Zhang, S., Song, D., Zhai, Y., …, & Liu, N. (2023). Ultra-conductive and transparent epidermal electrodes for simultaneous dual-mode assessment of brain function. *Chemical Engineering Journal*, *476*, 146628. https://doi.org/10.1016/j.cej.2023.146628

[103] Lee, S., Shin, Y., Kumar, A., Kim, K., & Lee, H. N. (2019). Two-wired active spring-loaded dry electrodes for EEG measurements. *Sensors*, *19*(20), 4572. https://doi.org/10.3390/s19204572

[104] Frey, S., Lucchini, M. A., Kartsch, V., Ingolfsson, T. M., Bernardi, A. H., Segessenmann, M., …, & Cossettini, A. (2025). GAPses: Versatile smart glasses for comfortable and fully-dry acquisition and parallel ultra-low-power processing of EEG and EOG. *IEEE Transactions on Biomedical Circuits and Systems*, *19*(3), 616–628. https://doi.org/10.1109/TBCAS.2024.3478798

[105] Ilkal, S. N., Munshi, S. S., Katarki, S., Kotwal, N., Chikkond, M., & Makandar, A. (2025). AI based facial recognition smart glass for visually impaired person. *Saudi Journal of Engineering and Technology*, *10*(06), 270–276. https://doi.org/10.36348/sjet.2025.v10i06.003

[106] Kaveh, R., Schwendeman, C., Pu, L., Arias, A. C., & Muller, R. (2024). Wireless ear EEG to monitor drowsiness. *Nature Communications*, *15*(1), 6520. https://doi.org/10.1038/s41467-024-48682-7

[107] Song, E. (2023). Soft, biocompatible materials and skin-like electronics as wearable devices: An interview with John A. Rogers. *National Science Review*, *10*(1), nwac191. https://doi.org/10.1093/nsr/nwac191

[108] Lee, B., Cho, H., Jeong, S., Yoon, J., Jang, D., Lee, D. K., …, & Hong, Y. (2022). Stretchable hybrid electronics: Combining rigid electronic devices with stretchable interconnects into high-performance on-skin electronics. *Journal of Information Display*, *23*(3), 163–184. https://doi.org/10.1080/15980316.2022.2070291

[109] Xu, W., Cao, Y., Shi, H., Jia, X., Zheng, Y., Tan, Z., …, & Wu, H. (2025). Skin-interfaced sweat monitoring patch constructed by flexible microfluidic capillary pump and Cu-MOF sensitized electrochemical sensor. *Talanta*, *291*, 127895. https://doi.org/10.1016/j.talanta.2025.127895

[110] Zhang, Y., Li, Z., Fan, X., Liu, Y., Li, Z., Zheng, Z., …, & Mou, L. (2025). A fully integrated, non-invasive, and multimodal wearable device for sweat stimulation, collection and multiple physiological signals analysis. *Chemical Engineering Journal*, *505*, 159209. https://doi.org/10.1016/j.cej.2025.159209

[111] Srikantaprasad, G., & Mathew, N. T. (2023). Fabrication of microchannels for microfluidic devices using laser micromachining. *Materials Today: Proceedings*. Advance online publication. https://doi.org/10.1016/j.matpr.2023.08.289

[112] Hossain, M. I., Zahid, M. S., Chowdhury, M. A., Hossain, M. M. M., Hossain, N., Islam, M. A., & Mobarak, M. H. (2024). Smart bandage: A device for wound monitoring and targeted treatment. *Results in Chemistry*, *7*, 101292. https://doi.org/10.1016/j.rechem.2023.101292

[113] Yu, Y. (2025). *Managing complex intelligent systems: The coexistence of generativity and criticality*. Sweden: Linköping University Electronic Press. https://doi.org/10.3384/9789180759984

[114] Eltholth, A. A. (2023). Improved spectrum coexistence in 2.4 GHz ISM band using optimized chaotic frequency hopping for

Wi-Fi and Bluetooth signals. *Sensors*, *23*(11), 5183. https://doi.org/10.3390/s23115183

[115] Yoo, S., Kim, S., Kim, E., Jung, E., Lee, K. H., & Hwang, H. (2018). Real-time location system-based asset tracking in the healthcare field: Lessons learned from a feasibility study. *BMC Medical Informatics and Decision Making*, *18*(1), 80. https://doi.org/10.1186/s12911-018-0656-0

[116] Edemekong, P. F., Annamaraju, P., Afzal, M., & Haydel, M. J. (2024). Health Insurance Portability and Accountability Act (HIPAA) compliance. In *StatPearls*. StatPearls Publishing.

[117] Al-Fuqaha, A., Guizani, M., Mohammadi, M., Aledhari, M., & Ayyash, M. (2015). Internet of things: A survey on enabling technologies, protocols, and applications. *IEEE Communications Surveys & Tutorials*, *17*(4), 2347–2376. https://doi.org/10.1109/COMST.2015.2444095

[118] Kinghorn, A. D. (2004). Quality standards of Indian medicinal plants, Vol. 1 A. K. Gupta, coordinator (medicinal plants unit, Indian Council of Medical Research). Indian Council of Medicinal Research, Ansari Nagar, New Delhi, India. 2003. xvii + 262 pp. 20 × 27. 5 cm. $40. 00. ISBN-0972-7213. *Journal of Natural Products*, *67*(4), 739–740. https://doi.org/10.1021/np030714y

[119] Schlauderaff, A., & Boyer, K. C. (2019). An overview of Food and Drug Administration medical device legislation and interplay with current medical practices. *Cureus*, *11*(5), e4627. https://doi.org/10.7759/cureus.4627

[120] Aldosari, B. (2025). Cybersecurity in healthcare: New threat to patient safety. *Cureus*, *17*(5), e83614. https://doi.org/10.7759/cureus.83614

[121] Contardi, M. (2019). Changes in the medical device's regulatory framework and its impact on the medical device's industry: From the medical device directives to the medical device regulations. *Erasmus Law Review*, *12*(2), 166–177. https://doi.org/10.5553/ELR.000139

[122] Krzysztofek, M. (2019). *GDPR: General Data Protection Regulation (EU) 2016/679: Post-reform personal data protection in the European Union*. Netherlands: Wolters Kluwer.

[123] Sharma, D., & Chandra, A. (2020). Medical device rules-2017, India: An insight. *Applied Clinical Research, Clinical Trials and Regulatory Affairs*, *7*(2), 126–134. https://doi.org/10.2174/2666255813666190912114043

[124] Garima, & Shreya. (2025). Data privacy and security in a globalized digital world: Legal perspectives on cross-border data flows. *Journal of Informatics Education and Research*, *5*(3), 1–14. https://doi.org/10.52783/jier.v5i3.3188

[125] Guided Solutions. (n.d.). *FDA clears Propeller Health sensor to work with Symbocort inhaler*. https://www.gsmedtech.com/GS/NewsDetails/FDA-clears-Propeller-Health-sensor-to-work-with-Symbocort-inhaler

[126] Julme, S., & Khan, M. (2025). Pharmaceutico-analytical standardisation of *Tripurabhairava Rasa* and evaluation of its acute oral toxicity, antipyretic, and analgesic activities in Wistar albino rats: A research protocol of experimental study. *Journal of Clinical & Diagnostic Research*, *19*(7), FK01–FK05. https://doi.org/10.7860/JCDR/2025/73537.21213

How to Cite: Kaur, S., Acharjee, T., Das, D., Bhatia, M., Sharma, S., Patel, A., & Bhatia, D. (2025). Switching on Smart Care: The Ascendancy of Wireless Technologies in Continuous Health Surveillance. *Smart Wearable Technology*, *1*, A13. https://doi.org/10.47852/bonviewSWT52026811